University of Nebraska - Lincoln
DigitalCommons@University of Nebraska - Lincoln

Engineering Mechanics Dissertations & Theses

Mechanical & Materials Engineering, Department of

8-2010

Time Dependence of Self-Assembly Process For the Formation of Inorganic-Organic Hybrid Nanolayers

Alexandre Dhôtel
University of Nebraska – Lincoln, alexandredhotel@gmail.com

Follow this and additional works at: https://digitalcommons.unl.edu/engmechdiss

 Part of the Mechanical Engineering Commons, and the Nanoscience and Nanotechnology Commons

Dhôtel, Alexandre, "Time Dependence of Self-Assembly Process For the Formation of Inorganic-Organic Hybrid Nanolayers" (2010). *Engineering Mechanics Dissertations & Theses*. 10.
https://digitalcommons.unl.edu/engmechdiss/10

This Article is brought to you for free and open access by the Mechanical & Materials Engineering, Department of at DigitalCommons@University of Nebraska - Lincoln. It has been accepted for inclusion in Engineering Mechanics Dissertations & Theses by an authorized administrator of DigitalCommons@University of Nebraska - Lincoln.

TIME DEPENDENCE OF SELF-ASSEMBLY PROCESS FOR THE FORMATION OF INORGANIC-ORGANIC HYBRID NANOLAYERS

by

Alexandre Dhôtel

A THESIS

Presented to the Faculty of

The Graduate College at the University of Nebraska

In Partial Fulfillment of Requirements

For the Degree of Master of Science

Major: Engineering Mechanics

Under the Supervision of Professor Li Tan

Lincoln, Nebraska

August, 2010

TIME DEPENDENCE OF SELF-ASSEMBLY PROCESS FOR THE FORMATION OF INORGANIC-ORGANIC HYBRID NANOLAYERS

Alexandre Dhôtel, M.S.

University of Nebraska, 2010

Advisor: Li Tan

There is increasing interest in self-assembled materials for energy storage, flexible electronics and hydrophobic barriers. Inorganic/organic hybrid thin films and especially organosilane-based coatings already have demonstrated their ability to achieve those goals. However, some fundamental points of their formation process by molecular self-assembly remain unexplained. Although the literature widely reports the effect of temperature on the final nanostructure, until now, no one has taken into account the importance of time during their synthesis.

The main objective of this study was to improve and complete the understanding of mechanisms responsible for the self-organization of organic/inorganic molecules into a highly ordered, layered structure. Indeed, by including gelation time as the main parameter during the preparation of

nanostructured films, we have shown that it is among the major criteria controlling molecular conformation.

By completing this research, we have filled a gap in the knowledge concerning the time dependence of the preparation of self-assembled molecules. We expect this work to be of general interest to all material engineers wanting to synthesize and control the internal structure of inorganic/organic hybrid thin films.

ACKNOWLEDGMENTS

I would like to express my gratitude to my advisor, Dr. Li Tan, for his continuous enthusiasm, guidance and encouragement throughout this project. He was abundantly helpful and understanding and offered me the opportunity to acquire valuable experiences.

I also would like to thank Lucia Fernandez-Ballester with whom I worked closely on this project and whose motivation and advice always inspired me to go further.

I gratefully thank Dr. Mehrdad Negahban and Pr. Jean-Marc Saiter from the University of Rouen for giving me the chance to take part in the EMME program and study under the best conditions. Without them, this great adventure would not have been possible.

Dr. Wonyoung Choe and Dr. Joseph Turner deserve a special thanks as my thesis committee members.

Sincere thanks to all the persons who helped me throughout this study, especially Chichao Yu, Mickael Arnoult, Jinyue Jiang, Sara Basiaga, Pinaki Mukherjee, Ziguang Chen, Carrie Shipers and Hualong Du.

Thanks to the FACE-PUF program for the financial support.

Last but not least, I really appreciated the support from all my family, my friends and my girlfriend in France throughout this year. They are greatly involved in the successful realization of this thesis.

TABLE OF CONTENTS

LIST OF FIGURES

Chapter 1: Introduction

Nowadays, the development and understanding of nanotechnologies have an important position in the scientific world. The concrete expression of this desire to manipulate matter on an atomic or molecular scale is recent and received a boost in the early 1980s with the birth of cluster science and the invention of the scanning tunneling microscope (STM) (1). Nanotechnologies can be divided into several domains; nanoelectronics, molecular self-assembly and nanomedicine are a few of them. For this study, we focused on the molecular self-assembly of organosilane molecules for forming inorganic/organic hybrid thin films. This kind of coating already has demonstrated its ability to produce novel hybrid materials with unique structures and properties (2) (3). Although they have found many applications in the fields of flexible electronics, hydrophobic barriers and energy storage, some aspects of their self-organization into a highly-ordered, layered structure remains unexplained.

The main challenge of this study was to fill a gap in the knowledge concerning the time dependence of film preparation and to gain a better understanding of the self-assembly process in order to control the internal nanostructure. We expect this work to be of general interest to all material engineers wanting to produce and control properties of hybrid thin films.

1.1 Background of molecular self-assembly

Molecular self-assembly is now known as a promising technique for the construction of highly-ordered structures without guidance from an outside template. Products formed through this process can exhibit remarkable properties, especially in the fields of opto-electronics (4), hydrophobic coatings (5), or sensors (6). Molecular self-assembly may be defined as the spontaneous organization of molecules from a disordered state so as to maximize the interactions between molecules and minimize the energy of the global system. The main advantage of this process is its reversibility. Indeed, molecules involved in self-assembled aggregates first are joined by non-covalent bonds, such as hydrogen bonding, Π-Π interactions or Van der Waals forces. This characteristic allows self-assembled structures to be dynamic. For instance, a damaged structure where a few weak bonds are broken can reassemble and repair itself due to constant intermolecular interactions (7). Another interesting aspect of molecular self-assembly is the possibility of generating structures in a range of sizes (~1.10^2 nanometers) that are hardly accessible through usual chemical synthesis routes (8). Since this technique uses elemental pieces to form a higher scale system, it is referred to as a "bottom-up" design in contrast to a "top-down" approach where an overall system is divided into its compositional sub-systems. The self-organization of organosilane molecules (R-SiX_3, R = C_nH_{2n+1} and X = OR or Cl) has been studied widely, particularly for the formation of superhydrophobic coatings due to the elevated surface roughness of films (9).

When dissolved in an appropriate solvent, organosilane can form well-ordered, layered nanostructures via hydrolysis, which enhances the polarity of molecules and leads to their clustering, and then the three-dimensional structures will be held due to condensation reactions which create covalent bonds (10). For such systems, the enhancement of the polarity of molecules by hydrolysis is the central point for their assembly. In fact, even though the total charge on a molecule is zero, the intrinsic structure and composition of the molecule may lead to the appearance of positive and negative charges in few places. Basically, polarity refers to an asymmetric distribution of electric charge in a molecule due to an unequal sharing of electron density between atoms. One can picture this characteristic like creating an electrostatic field surrounding the molecule (Figure 1). When polar molecules are close enough, opposite charges carried by molecules are attracted just like with magnets. Depending on the charge distribution throughout the molecules and the environmental conditions, they may form an ordered structure. For the self-assembly of organosilane molecules, the hydrolysis process is essential since it forms many –OH groups in the molecule, which greatly increase its polarity.

The formation of nanostructured materials through self-assembly is strongly dependent on experimental conditions such as temperature, concentration and the pH of the solution. Many efforts have been made to determine the best conditions for the self-assembly of organosilane molecules, depending on chemical compounds and desired structures (11) (12). However, the literature does not clearly report the effect of different gelation time (tg) on the internal structure of films.

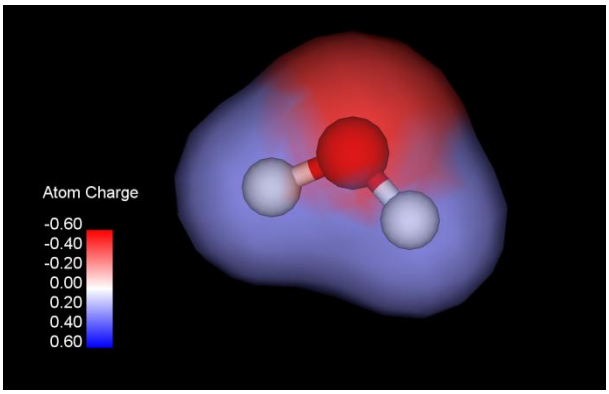

Figure 1. Modeling of a water molecule surrounded by its electrostatic field. Blue and red parts represent positive and negative charges respectively.

By definition, gelation time can be expressed as the time interval between the introduction of a catalyst into a liquid system and the formation of a gel (dilute crosslinked system).

1.2 Nanolayered structures

Self-assembled materials can be found under several forms such as micelles, vesicles, or layers (Figure 2). Those molecular configurations are often the result of the use of surfactants as building blocks.

As described above, the self-assembly process mainly relies on the difference in the polarity of the molecules, which may be attracted or rejected depending on their local charge. In the case of surfactants, one also can envisage this assembly as the result of hydrophobic interactions. Surfactants are compounds composed of two parts, a hydrophilic head to which is attached a hydrophobic tail. In fact, the

hydrophilic head is composed of atoms that exhibit strong dipole moments, which are absent in the hydrophobic tail.

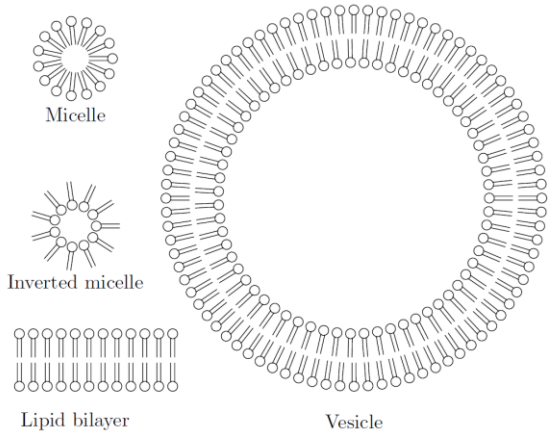

Figure 2. Schematic representations of micelles, vesicle and bilayers (13).

Basically, heads are designated as liking water and tails as hating water. Thus, when surfactants are dissolved into an aqueous environment the heads of molecules will try to increase their interactions with the solvent (water) while the tails will try to keep away from water. Thus, to minimize the energy of the overall system, hydrophobic tails gather, allowing them to reduce their contact with water as much as possible. This feature may lead to the formation of structures, as depicted above (Figure 2). Depending on the concentration of the solution, the atomic composition of the molecules and the type of solvent, the self-assembly process will result in the formation of a thermodynamically favorable conformation (14).

In this study, we are interested principally in the formation of layers (or lamellar structures). In the case of organosilane molecules the hydrophilic heads contain a central silicon atom (R-SiX_3 or SiX_4, R = C_nH_{2n+1} and X = OR or Cl) and the hydrophobic tails may be formed simply by alkyl chains. Thus, layers of organosilane molecules can be represented as an alternance of inorganic moieties (heads) separated by organic compounds (tails). Such systems often are designated as inorganic/organic hybrid thin films.

Many efforts to control the molecular packing of similar systems have been made by modifying the temperature of the reaction mixture or its composition (15) (16). Generally, they are used under their bilayered configuration even though sometimes interdigitated layers are formed. Schematic representations of those two common layered structures are depicted in Figure 3.

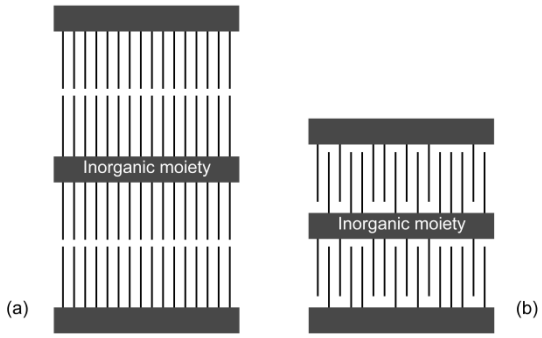

Figure 3. Schematic representation of (a) bilayers and (b) interdigitated layers.

By imagining the structures in Figure 3 as being surrounded by solvent, one clearly can picture that the hydrophilic moieties form like barriers to prevent the

organic tails from coming into contact with the solvent. Layered structures are not the most favorable molecular conformation for surfactants since, contrary to micelles or vesicles, they do not totally protect the organic tails from the solvent on the lateral edges. They are created when the building blocks are not adapted for the formation of vesicles or micelles. For instance, a building block composed of a too long tail attached to a small head would prevent the formation of globular structures (vesicles, micelles) and would prefer to form layered structures.

A bilayer might be described as a head-to-head arrangement of molecules. Their heights generally are close to twice the length of the constituent and their formation is dependent on several conditions, such as the length of the hydrophobic tail. Previous studies (11) (16), already have demonstrated the inability of amphiphilic molecules whose alkyl chains are too short (C_nH_{2n+1}, $n<14$) to self-assemble into well-defined bilayers due to the low extent of hydrophobic interactions.

Two potential ways of formation exist for interdigitated layers. On the one hand, they can appear due to a successive up and down organization of molecules. Basically, instead of having the stacking of two heads one above the other, as in bilayers, here the inorganic moieties are formed only by a simple alignment of heads. As for the tails, they are alternately pointing up or down in an *a priori* random fashion. On the other hand, the amphiphilic molecules can be spaced out because of the intercalation of additional molecules in the inorganic moiety which will create a

larger gap between hydrophobic tails. Thus, those gaps can be filled by the tails of neighboring layers (17), as one can interlock one's fingers. In those layered structures of organosilane, bilayers as well as interdigitated layers, molecules first are held together by weak bonds (hydrogen bonds), and then condensation reactions create covalent bonds which make the structures more robust but also irreversible.

1.3 Motivation

According to its definition, gelation time (tg) should be considered among the major parameters controlling the process of molecular self-assembly. Nevertheless, to the best of our knowledge, the relationship between gelation time and the internal structure of self-assembled organosilane molecules has not been examined yet. By conducting this study, we wanted to obtain an understanding of the self-assembly process of a molecular system frequently used in water-repellent coatings. This knowledge may provide the basis for fine-tuning the final morphology and properties obtained by controlling the pathway of self-assembly.

For example, an equivalent system already has shown remarkable hydrophobic properties with a contact angle going up to 152° (18). Those properties are due both to the intrinsic composition of molecules and to their conformation which creates a rough surface essentially composed of carbon atoms. Therefore, one can envisage that better control of the molecular packing could result in either better hydrophobic properties or superior thermal or aging stability.

We expect this study to illuminate a fundamental point of the self-assembly process for organosilane molecules, which could be perceived as a complement to the literature by all material engineers having the desire to control precisely the internal nanostructure of their films.

Chapter 2: Experimental Section

This study proposes to analyze the self-assembly mechanisms of a unique system composed of two organosilane molecules, i.e., Hexadecyltrimethoxysilane (HDTMS) and Tetramethoxysilane (TMOS), whose molecular structures are depicted in Figure 4. Their linear chemical formulas are $H_3C(CH_2)_{15}Si(OCH_3)_3$ and $Si(OCH_3)_4$, respectively.

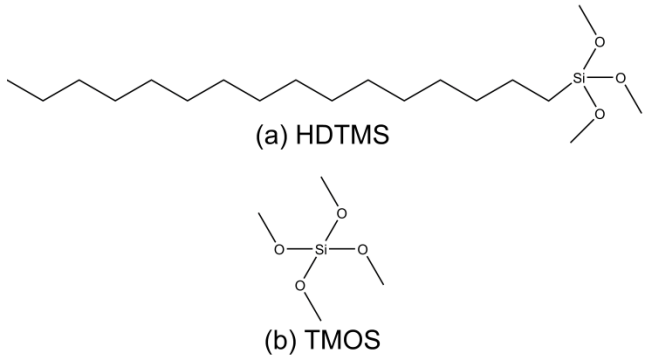

Figure 4. Molecular structures of (a) HDTMS and (b) TMOS

HDTMS is an amphiphilic molecule; its hydrophilic head is composed of a central silicon atom to which is attached three $-OCH_3$ groups, and its hydrophobic tail is constituted of an alkyl chain formed by a straight succession of fifteen CH_2 groups and one CH_3 group at its end. The molecular structure of TMOS is close to HDTMS; the only difference is that the alkyl chain is replaced by a fourth $-OCH_3$ group.

2.1 Materials

Hexadecyltrimethoxysilane (technical, ≥85%) was purchased from Fluka. Tetramethoxysilane (≥99%), hydrogen peroxide and sulfuric acid were purchased from Sigma-Aldrich. Tetrahydrofuran (THF) was purchased from Fisher Scientific. All chemicals were used as received without further purification. The 4" P(100) 10-20 ohm-cm SSP 500 um Prime Grade and 4" P(100) 1-10 ohm-cm DSP 500 um Prime Grade silicon wafers were purchased from University Wafer. After being cut into rectangular pieces (~1x1.5cm) they were brushed with water, sonicated for 15 minutes in ethanol, then in acetone and treated with an acidic solution composed of H_2SO_4:H_2O_2 = 1:1 (volume ratio) for 30 minutes in order to increase the number of Si-OH groups on their surfaces. After treatment, they were rinsed several times in water then dried with nitrogen.

2.2 Reaction procedure

Hexadecyltrimethoxysilane (HDTMS) was added to a mixture of Tetrahydrofuran (THF), water, and hydrochloric acid. The reaction mixture was stirred at 400 RPM for 3 hours at room temperature; then Tetramethyl orthosilicate (TMOS) and an additional amount of water were added. The initial composition of the mixture was HDTMS:TMOS:THF:H_2O:HCL = 1:1:100:7:0.002 (molar ratio). The resulting solution was dropcasted onto a piece of silicon wafer and dried in a covered petri dish for 24 hours at room temperature. The time gap between the

addition of TMOS and the dropcasting of the solution on the silicon wafer was defined as the gelation time (t_g) and varied between 1 minute and 24 hours.

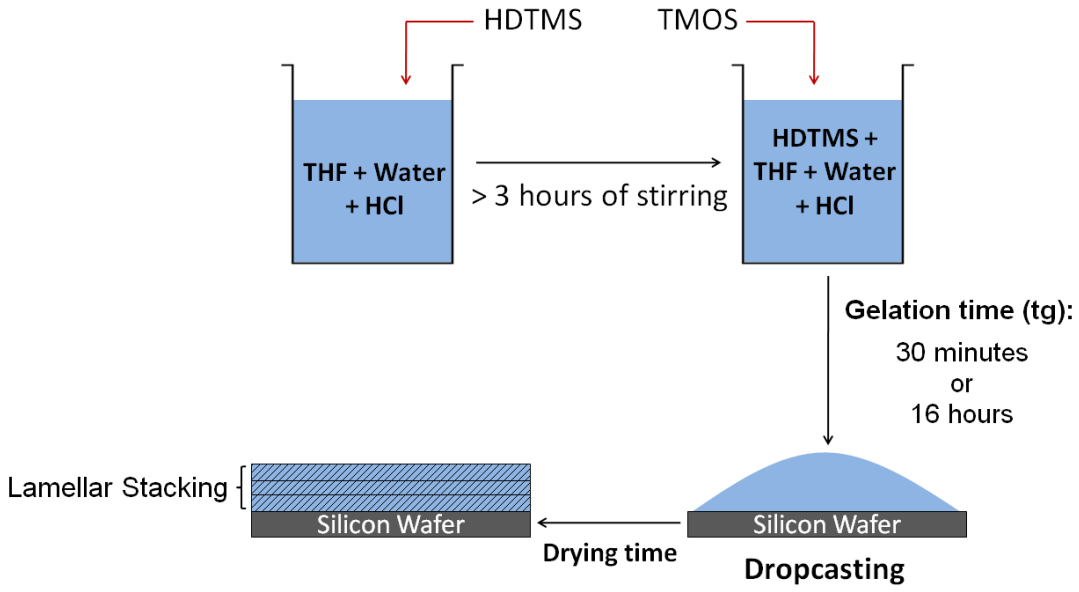

Figure 5. Schematic representation of the preparation process of the HDTMS + TMOS solution.

Fresh samples were stored 1 day after drying while aged samples were stored for 10 days. The storing was performed at room temperature and pressure, and the films were covered by a cap in order to protect them from dust. The solution was stirred quickly by hand before being dropcasted in order to make it homogeneous. Figure 6 shows a fresh thin film whose t_g = 30 minutes.

Figure 6. Picture of a fresh film composed of HDTMS and TMOS dropcasted onto a silicon wafer, tg = 30minutes

2.3 Characterization

Wide and small X-Ray diffraction patterns were obtained on a Rigaku D/Max-B Geigerflex diffractometer using a Cu Kα (~1.544 Å) radiation and a graphite monochromator. Digital data were recorded for a 2θ range 1-28° at an angular resolution of 0.02°. The films were analyzed directly on their silicon substrate at an angular velocity of 0.5°/min. Small-angle X-Ray scattering (SAXS) was recorded from 1° to 14° on very thin films (~ few microns). Wide-angle X-Ray scattering (WAXS) was recorded from 18° to 28° on thicker films (~ 1 mm). The Atomic Force Microscope (AFM) Dimension 3100 SPM was used at room temperature to obtain topographic images of the films and highlight the layered structure. Images were recorded at a maximum resolution of 512 samples/line. Thermogravimetric Analyses (TGA) and Differential Scanning Calorimetry analyses (DSC) were performed by a STA 6000 (simultaneous thermal analyzer) from Perkin Elmer through use of an internal reference balance. TGA/DSC measurements were made from 25 to 800°C at a heating rate of 5°C/min under a nitrogen flow. The data were recorded at 0.03°C

intervals. The FTIR-ATR spectra were recorded by a Nicolet Avatar 360 FT-IR with a SmartPerformer ATR assembly. This machine utilizes a zinc selenide (ZnSe) ATR lens that is IR transparent through 500 cm^{-1}. Acquisitions were performed at a resolution of 4 cm^{-1}. The films were scratched at the substrate surface before being analyzed. Optical microscope images were acquired on a Leica DM 2500M. Wettability tests were realized by using a high-speed digital CCD camera recording the free falling of drops at a frequency of 5000 frames per second. Water droplets were casted by a syringe 4.5 cm above the surface of films.

Chapter 3: Results and Discussion

Many efforts have been made in order to control the molecular conformation of a wide range of self-assembled organosilane molecules with intent of controlling their mechanical, hydrophobic or thermal properties (15) (11). The HDTMS + TMOS system (or its equivalent) already has demonstrated its abilities to form tunable ordered nanostructures by varying temperature during the preparation process (15). However, numerous parameters have an impact on the formation of self-assembled films. The main objective of the present study is to explore another key parameter, the gelation time, and use it to understand the hydrolysis and condensation processes occurring during film preparation. Thus, one would be able to control the nanostructural arrangement of molecules and therefore their properties.

3.1 Hydrolysis and condensation of precursors

The self-organization of HDTMS and TMOS is the consequence of two processes which occur throughout the preparation process of films. On the one hand, the amphiphilic nature of HDTMS molecules containing both a hydrophilic head, i.e. ($Si(OCH_3)_3$), and a hydrophobic tail, i.e. ($C_{16}H_{33}$), creates local hydrophobic interactions, leading molecules to organize themselves into a lower free energy state. On the other hand, when hydrolyzed molecules are close enough they condense and form stronger covalent bonds, allowing them to maintain the newly formed structure. Those processes are very effective for the formation of silica-organic nanostructured materials by self-assembly.

The main consequence of the hydrolysis is an increase in the polarity of molecules which amplifies local hydrophobic interactions. Indeed, in this particular case, hydrolysis splits the SI-O-CH_3 groups contained in the TMOS and HDTMS head and forms SI-OH groups (19) (18) whose polarity is superior. The hydrolysis reactions of HDTMS and TMOS can be expressed as follows:

TMOS hydrolysis:

$$\mathrm{Si(OCH_3)_4 + 4H_2O \rightarrow Si(OH)_4 + 4CH_3}OH$$

HDTMS hydrolysis:

$$\mathrm{C_{16}H_{33}Si(OCH_3)_3 + 3H_2O \rightarrow C_{16}H_{33}Si(OH)_3 + 3CH_3}OH$$

One can remark the formation of methanol ($\mathrm{CH_3}OH$ or abbreviated MeOH) as a residue of the hydrolysis of HDTMS and TMOS. Due to its high toxicity for humans (ingestion of 10 mL can cause permanent blindness and 30 mL can be fatal), most researchers prefer to work on equivalent systems but creating ethanol ($\mathrm{C_2H_5}OH$ or abbreviated EtOH), which is healthier. One can see clearly on Figure 7 the enhancement of HDTMS and TMOS polarities after hydrolysis. White shades represent neutral parts of molecules while blue and red shades indicate the charged sections of molecules.

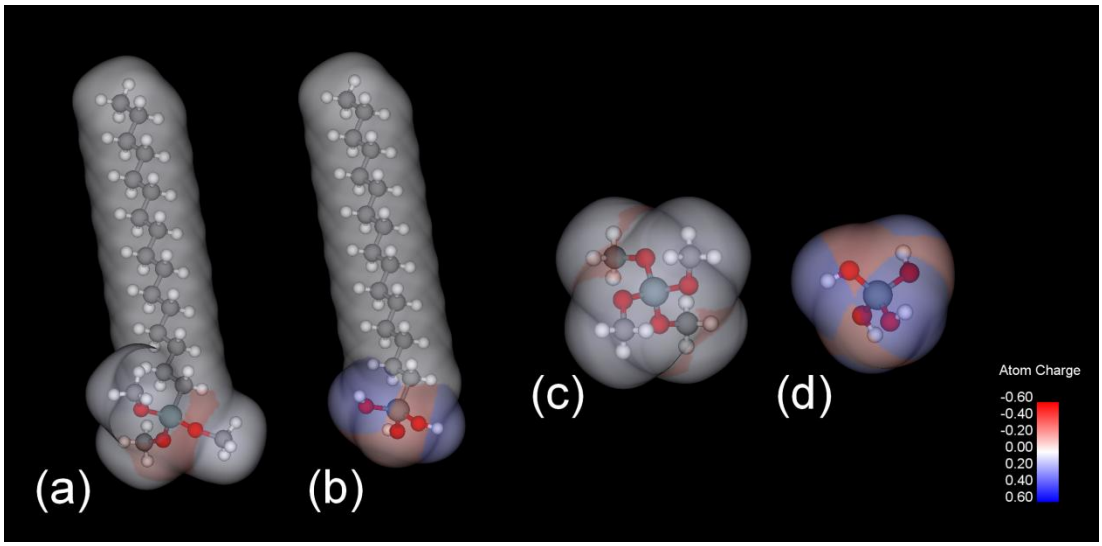

Figure 7. Enhancement of molecular polarity by hydrolysis, (a) non-hydrolyzed HDTMS, (b) hydrolyzed HDTMS, (c) non-hydrolyzed TMOS, (d) hydrolyzed TMOS. Blue and red shades represent positive and negative charges respectively.

Although hydrolysis enhances the polarity of the entire molecule of TMOS, in the case of HDTMS the increase in polarity is located in the inorganic head only and the tail is not affected. This characteristic is what defines HDTMS as an amphiphilic molecule. As described in Chapter 1, to self-assemble those molecules must be dissolved in a polar solvent. Since the use of water as a solvent would hydrolyze molecules too rapidly and would be a limiting factor for the drying and formation of films due to its elevated boiling point, THF was used for its good polar properties combined with a relatively low melting point (~66°C). After hydrolysis and due to the increase in the polarity, intermolecular hydrophobic interactions are amplified. Therefore, depending on the local charges of molecules, they are either attracted to or repulsed by each other, with the negative end of one molecule

attracting the positive end of another. Hydrophobic interactions lead to the formation of ordered structures where each part of the molecules are packed in order to satisfy a low free energy state; thus hydrophobic tails are gathered next to each other while hydrophilic parts create a sort of barrier surrounding tails so as to protect them from water or other polar components.

When molecules are close enough they are linked by electrostatic forces (hydrogen bonds) as a first step. This characteristic allows a certain reversibility of the structure thanks to the weakness of hydrogen bonds, which easily can be broken and reformed afterwards. Thus, if a structure does not well satisfy a stable state it can be rearranged. After being linked by weak bonds, molecules tend to create stronger chemical bonds (polar covalent bonds) by sharing of valence electrons which causes a more stable electronic configuration. This reaction is called condensation and prevents the reversibility of the structure. Indeed, the range of energies for a covalent single bond is equal to 200-500 kJ/mol while for hydrogen bonds the energies range from 10 to 40 kJ/mol (20). Therefore covalent bonds need much more energy to be broken than hydrogen bonds.

The condensation reactions of HDTMS and TMOS can be expressed as follows (21):

TMOS water condensation:

$$\mathrm{nSi(OH)_4 \rightarrow nSiO_2 + 2nH_2O}$$

TMOS alcohol condensation:

$$Si(OH)_4 + Si(OCH_3)_4 \rightarrow HO-\underset{\underset{OH}{|}}{\overset{\overset{OH}{|}}{Si}}-O-\underset{\underset{CH_3}{|}}{\overset{\overset{CH_3}{|}}{\underset{\underset{O}{|}}{\overset{\overset{O}{|}}{Si}}}}-O-CH_3 + CH_3OH$$

HDTMS water condensation:

$$2C_{16}H_{33}Si(OH_3) \rightarrow C_{16}H_{33}\underset{\underset{OH}{|}}{\overset{\overset{OH}{|}}{Si}}-O-\underset{\underset{OH}{|}}{\overset{\overset{OH}{|}}{Si}}C_{16}H_{33} + H_2O$$

$$HDTMS\ alcohol\ condensation:$$

$$C_{16}H_{33}Si(OH)_3 + C_{16}H_{33}Si(OCH_3)_3 \rightarrow C_{16}H_{33}\underset{\underset{OH}{|}}{\overset{\overset{OH}{|}}{Si}} - O - \underset{\underset{CH_3}{|}}{\overset{\overset{CH_3}{|}}{Si}} C_{16}H_{33} + CH_3OH$$

One can remark that alcohol condensations occur when a non-hydrolyzed part of a molecule condenses with another one that is hydrolyzed already while water condensations occur when the two condensing parts of the molecules are hydrolyzed already.

In general, the gelation time (t_g) might be defined as the time interval between the beginning of the hydrolysis and the end of condensation; however, in our particular case we focused on the gelation time for TMOS molecules only. Thus, t_g starts as soon as TMOS is inserted into the reaction mixture and ends when the solution is casted onto a silicon wafer. This parameter represents a remarkable advantage for the understanding of self-assembly mechanisms. Indeed, by varying this parameter one easily can determine what is happening into the reaction mixture step by step and thus one can identify each mechanism responsible for the formation of films and when it occurs.

The decision to use silicon wafers treated by an acidic solution as a substrate for the films was made in order to increase the interactions between molecules in the

solution and the substrate surface. After acidic treatment the surface of the substrate reveals the presence of numerous Si-OH groups. Those groups being polar the surface becomes extremely hydrophilic which makes easier the spreading of the solution on the surface and the creation of bonds between HDTMS, TMOS and Si-OH groups of the surface (Figure 8) (9). This condensation reaction may cause the formation of water molecules or CH_3OH groups.

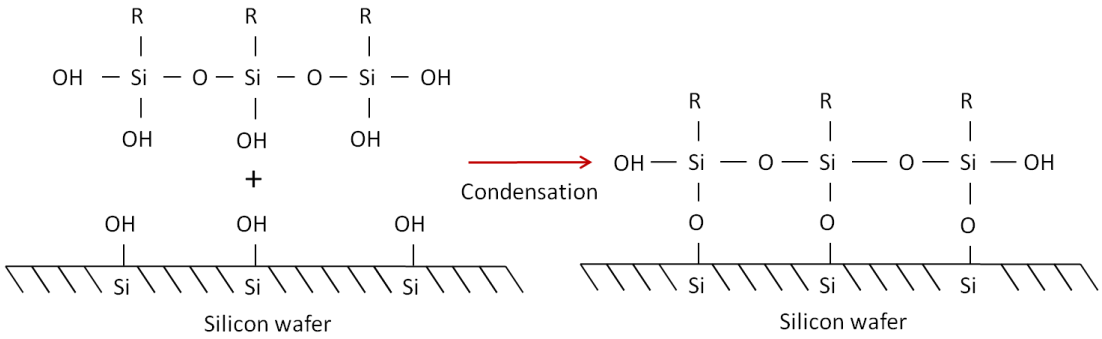

Figure 8. Condensation of molecules on silicon wafer.

3.2 X-Ray Diffraction (XRD)

The X-Ray diffraction of films made from a solution with a gelation time t_g = 30 minutes (Figure. 9) indicates the presence of a well defined layered structure α. The first order peak arises from the basal spacing of layers in the α phase, while the significant number of higher order diffraction peaks (up to n = 13) implies that the structure is very well-ordered. The basal spacing of 4.3 nm for the α phase is very close to twice the length of HDTMS molecules (2.3 nm) which suggests that the

layers are formed by a head-to-head arrangement of HDTMS ($C_{19}H_{42}$**SIO$_x$-O$_x$Si**$C_{19}H_{42}$), also called bilayers. Wide-angle diffraction shows an extra peak around 2θ = 20.5° (4.32 Å) which, in agreement with (19) (16) (17), is assigned to the spacing between alkyl chains in the α phase.

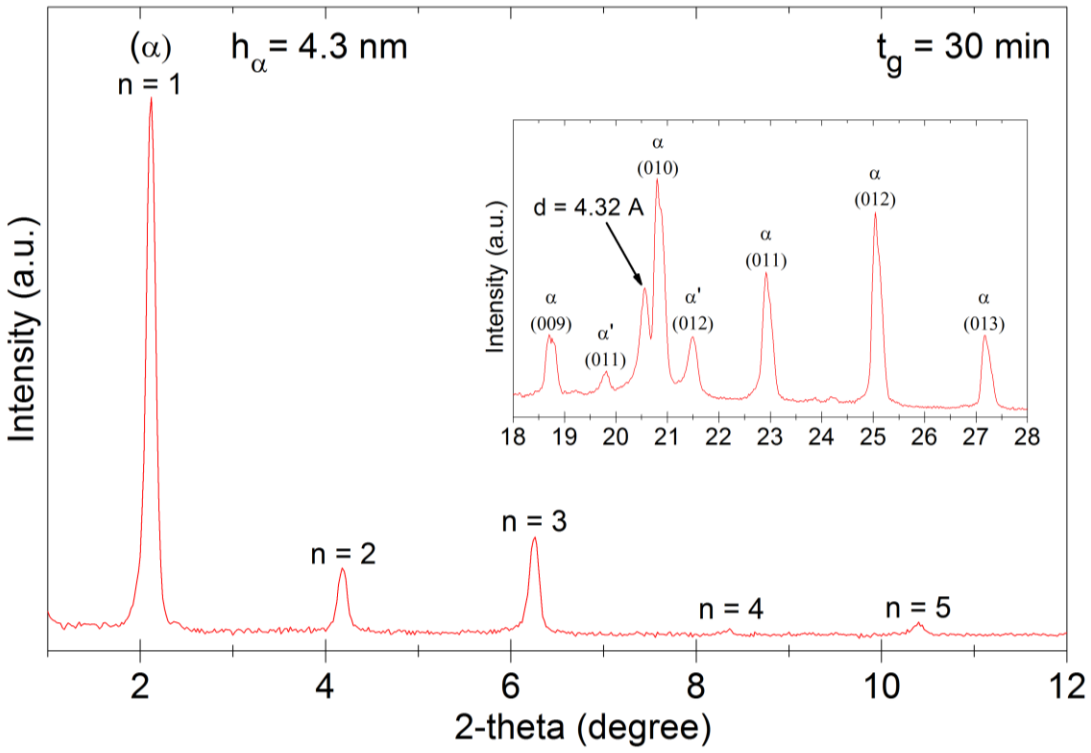

Figure 9. XRD patterns of HDTMS + TMOS films for t_g = 30 minutes. The specimen is composed of a single phase (α) with layer height of $h_α$ = 4.3 nm. Inset: wide angle X-ray diffraction peak at 4.32 Å assigned to the spacing between alkyl chains in the (α) phase.

Due to the significantly larger thickness of the samples used for WAXS (in order to obtain sufficient signal to noise ratio in the wide angle region), the inset of Figure 9 also shows the presence of a small quantity of α' phase in films. This

secondary phase is not observed in SAXS performed on thin films; therefore one can assume that this phase represents an insignificant part of films. However, this α' phase may appear while doing SAXS on thicker films (pattern available in Appendix A). One reason for the formation of α' bilayered phase whose basal spacing (4.8 nm) is larger than the α phase could be a distortion of the inorganic lattice (16). More specifically, this increase in the height of bilayers (~0.5 nm) might be the result of a turbostratic stacking of layers, in which adjacent basal planes can slip relative to each other (17). When planes have slipped, the gap between them is increased, causing a greater height of the global bilayers after slipping. Here, this behavior is made possible by the weakness of the hydrogen bonds which maintain the inorganic lattice.

This bilayered stacking is identical to the internal nanostructure of films prepared with a gelation time equal to 30 minutes but without TMOS (XRD pattern is available in Appendix A). According to A. Shimojima et al. (15) the high degree of hydrophobic interactions caused by the long alkyl chains of HDTMS encourages the condensation between HDTMS molecules and limits the creation of bonds with TMOS. Moreover, this characteristic is reinforced by the fact that during the preparation of the solution TMOS is added after the stirring of HDTMS molecules for 3 hours; thus HDTMS are able to start the formation of bilayers while TMOS molecules are not yet in the solution (cf. Figure. 5).

Since no evidence has been found of the presence of an ordered TMOS phase by X-Ray diffraction and the fact that HDTMS + TMOS films are similar to HDTMS films when t_g = 30 minutes, one might venture the hypothesis that TMOS had not enough time to interact with HDTMS molecules and may have formed an amorphous phase adjacent to HDTMS bilayers.

The sharpness of the diffraction peak corresponding to the spacing between alkyl chains at $2\theta = 20.5°$ suggests that molecules involved in bilayers are strictly parallel. Indeed, since a gelation time tg = 30 minutes is relatively short, one can assume that most of molecules involved in bilayers are still held together by hydrogen bonds only. Those bonds being weak, molecules do not undergo strong deformation or reorientation during the formation of layers. This characteristic also indicates that the condensation of molecules has not occurred yet and therefore this system is still reversible.

The stability of films formed from a solution with a gelation time tg = 30 minutes was tested by doing XRD experiments on a specimen aged 10 days (XRD pattern available in Appendix A). This experiment has revealed a phase transition from α to α’ over time. Indeed, after aging the α’ phase becomes visible on SAXS patterns which, in agreement with (17), could indicate that a part of the α phase has undergone a slipping leading to a higher basal spacing. This slipping was made possible due to the weakness of hydrogen bonds which are broken and then reformed after the slipping. However, the reproducibility of this feature needs to be confirmed.

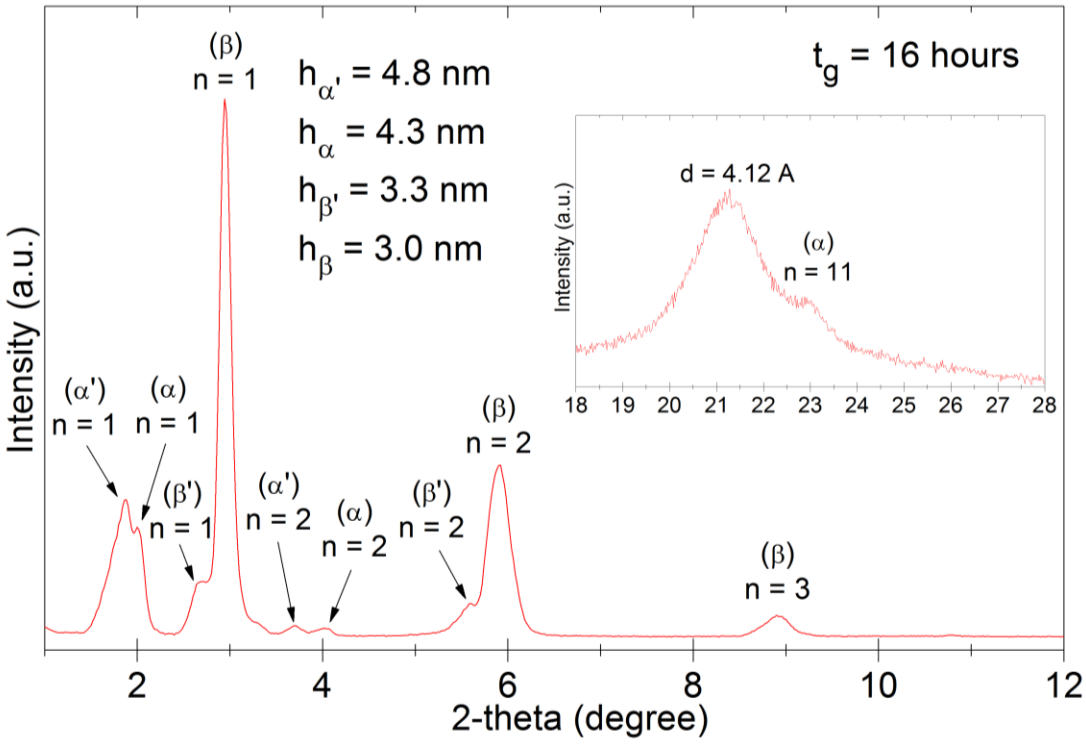

Figure 10. XRD patterns of HDTMS + TMOS films for tg = 16 hours indicate multiple phases: α', α, β', β of basal spacing 4.8 nm, 4.3 nm, 3.3 nm and 3.0 nm, respectively. Inset: WAXS shows the presence of two peaks at 2θ ~ 21.2° and 2θ ~ 23°.

A longer gelation time (t_g = 16 hours) has an important impact on the internal conformation of HDTMS + TMOS molecules. Indeed, X-Ray diffraction patterns on Figure 10 reveal the presence of four different types of structures. The presence of α' and α phases already encountered in films of short gelation time (30 minutes) indicates the film as being composed partially of HDTMS bilayers but according to the relative intensities of the peaks, one can assume that the films are composed primarily of a new phase β. This nanostructure composed of multiple phases strongly differs from the structure of films obtained with a similar gelation time but on a

system without TMOS (XRD pattern available in Appendix A). Indeed, in the case of films formed only from HDTMS, the gelation time does not seem to affect the global molecular conformation of films and one gets only a stacking of bilayers α.

The height of those β and β' layers (3.0 and 3.3 nm respectively) are too short to be considered as bilayers and too high to be assigned to simple HDTMS monolayers (tail-to-head stacking of molecules), so as proposed by A.B. Bourlinos et al., they were ascribed to interdigitated layers (17) (22). One explanation for the formation of such layers would be the effect of the intercalation of TMOS between HDTMS heads.

As observed above, the condensation of molecules is not immediate and takes time to occur. Before being completely condensed, structures are still reversible; thus molecules still are able to move in order to create a new configuration satisfying a lower free energy state. A good way to decrease the global free energy of a system is to create ordered structures. However, as revealed above, TMOS does not seem to be incorporated into bilayers when only a short gelation time is allowed. Therefore, to reach a lower free energy state, TMOS molecules tend to get integrated in the bilayers over time at the location where it is easier to do so (i.e., in their inorganic moieties where the heads of HDTMS are weakly linked). Since most of those heads are weakly bonded TMOS can break those bonds and intercalate between them, which increases the spacing between HDTMS molecules. If the gap between HDTMS molecules is large enough, the organic tails of neighboring layers can be

intercalated and fill those gaps. This interdigitation of alkyl chains may occur in order to minimize the Gibbs free energy of the system:

$$\Delta G = \Delta H - T\Delta S \quad (1)$$

where ΔG is the change of free energy, ΔH is the change of enthalpy, T is the temperature, and ΔS is the change of entropy.

In fact, according to equation (1) and considering an isothermal process, there exist two ways for the system to reduce its free energy. On the one hand, the system may rearrange its molecular configuration by undergoing exothermic reactions. Since the difference in enthalpy resulting from an exothermic reaction is negative then the ΔH term will be decreased. On the other hand, the system may increase its disorder. The entropy being a measure of the disorder within a system then by enhancing it the ΔS term will be increased. Therefore if the system forms a significant number of ordered structures during self-assembly then the overall free energy will be minimized.

Moreover, the second law of thermodynamics states that the entropy of an isolated system which is not in equilibrium will tend to increase over time. Thus the formation of ordered structures would violate this law since it tends to reduce the entropy of the system (Gibbs paradox). Thus, to respect the empirical postulate of the second law of thermodynamics, the “local” decreases in entropy caused by the formation of ordered structures will be associated with an increase in the “total”

entropy of the system. For instance, the system may increase the dissolution of molecules (23) leading to a thermodynamically favorable configuration. This increase in entropy will also participate to the decrease of the free energy of the system.

By the same token as for the α' phase, the β' phase could be ascribed to a part of the β phase which has slipped and increased its basal spacing (turbostratic stacking). This may explain the increase in the height (~0.5 nm) of β' compared to β.

WAXS on Figure 10 shows two peaks. The one at $2\theta \sim 23°$ (d = 3.9 A) corresponds to the 11^{th} order of the diffraction peak corresponding to the basal spacing of α phase. The peak at $2\theta \sim 21.2°$ (d = 4.12 A) then was assigned to the spacing between alkyl chains. The breadth of this peak can be explained by the condensation of molecules. Indeed, due to the directional character of covalent bonds which appear during the condensation, molecules have a tendency to come closer, bend and tilt, as shown in Figure 11. This distortion of the inorganic moiety results in a larger distribution of values for the spacing between alkyl chains and explains the lower average value for the spacing between chains.

Figure 11 highlights the difference in the conformation of molecules before and after condensation. This model was realized by taking into account HDTMS molecules only in order to be more explicit. However, this distortion of the inorganic moiety is observable in both cases, i.e., when films are formed from a solution with and without TMOS (WAXS pattern of HDTMS films in Appendix A).

In order to investigate the stability of films formed from a solution with a gelation time of 16 hours, XRD experiments were performed on films aged 10 days (XRD pattern available in Appendix A). The conformation of molecules did not change during that time interval; therefore one can guess that a long gelation time is favorable for the stability of films.

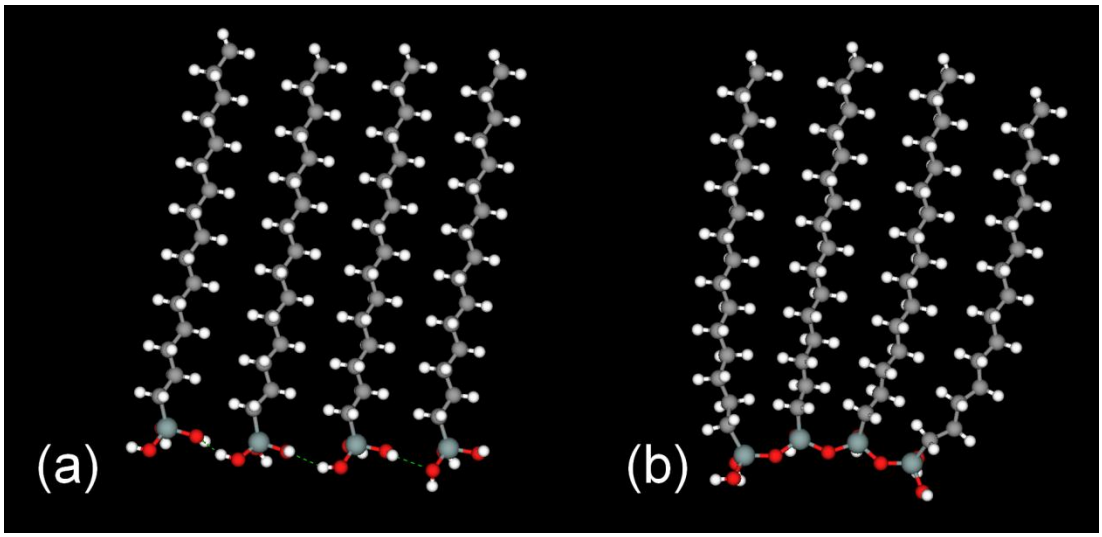

Figure 11. Distortion of the inorganic moiety after condensation. HDTMS molecules linked by (a) hydrogen bonds (green dashed lines), (b) by covalent bonds.

Moreover, a much longer gelation time (3 days) does not affect the final structure of the films. Thus, we assumed that 16 hours of gelation is suitable for molecules to reach their equilibrium state at room temperature and pressure.

In Figure 12, one clearly can see the formation of β phase over gelation time. This formation is accompanied with a decrease in the intensity of the peak corresponding to α phase. Thus, one can confirm that the β phase is formed from the

part of α phase which has not condensed yet and which consequently is able to form new interdigitated layers by incorporating TMOS.

Even though this figure shows an increase in the intensity of the peak corresponding to the basal spacing of the α phase between t_g = 1 minute and t_g = 6 hours, we cannot be sure that this tendency comes directly from the system. Indeed, the intensity of XRD peaks is dependent on many parameters, such as film thickness and surface of the specimen covered by the X-Ray beam, which cannot be accurately controlled here.

Nevertheless, a plot of the areas under the diffraction peaks corresponding to α and β phases as a function of gelation time was made (plot available in Appendix A). It may give a rough estimation of the relationship between the formation of interdigitated layers (β and β' phases) and the consequence on the amount of bilayers (α and α' phases) present in the films.

In order to confirm that after long gelation time, the condensation of molecules is completed, we have prepared a solution containing only HDTMS as building blocks. The solution was stored for 48 hours and then we added TMOS followed by a gelation time of 16 hours (the resulting XRD pattern is available in appendix A). As we expected, the film is only composed of bilayers α and α'. No peak related to the presence of interdigitated layers was observed.

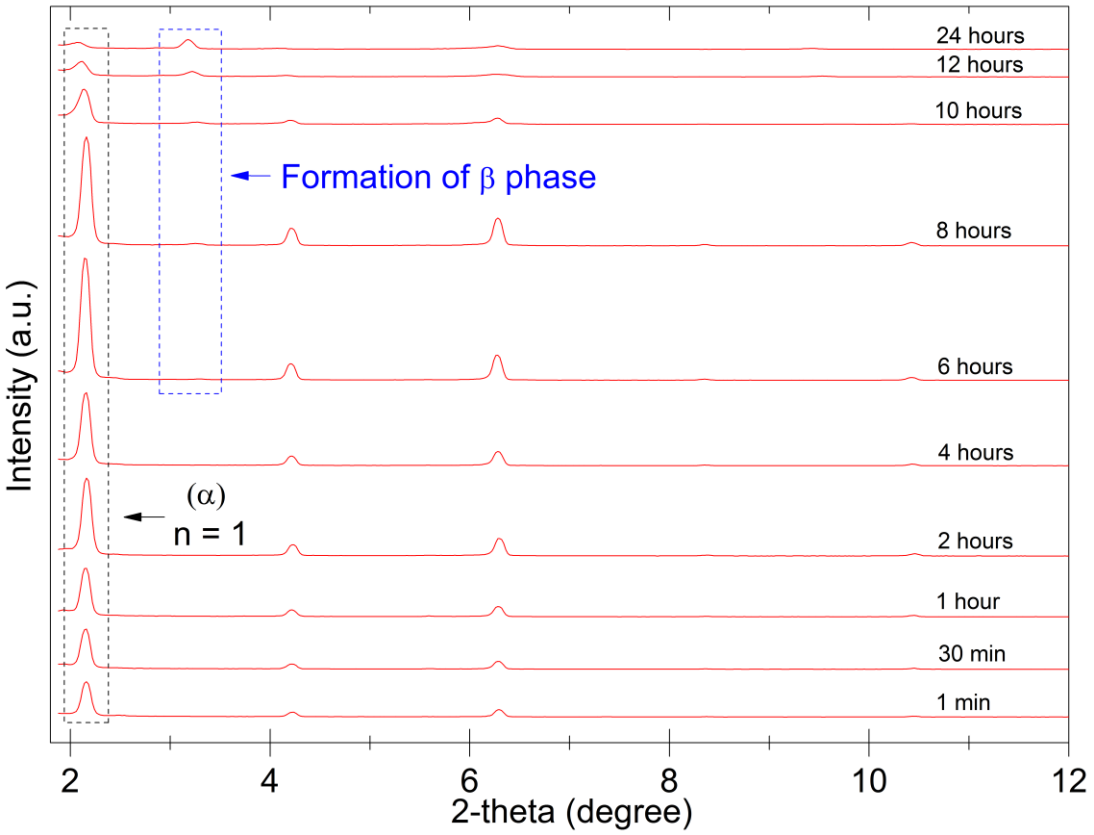

Figure 12. XRD patterns of HDTMS + TMOS with gelation time going from 1 min to 24 hours.

After 48 hours the condensation of molecules is completed, thus the structure is locked and prevents the insertion of TMOS in bilayers which would have caused the formation of interdigitated layers. However, the limited number of higher order diffraction peaks (up to n = 3) indicates that the internal structure of the film is not very well ordered. This might be explained by the disruptions caused by the strong interactions of TMOS molecules with the already formed HDTMS bilayers.

3.3 Atomic Force Microscopy (AFM) and Optical Microscopy

AFM images (Figure. 13) have highlighted the reliefs on the surface of the film. The layers easily can be seen as being stacked one on top of the others. The height profiles confirmed the presence of each type of layers (α', α, β' and β) by measuring their respective heights (only α and β layers are shown in the height profile of Figure 13.

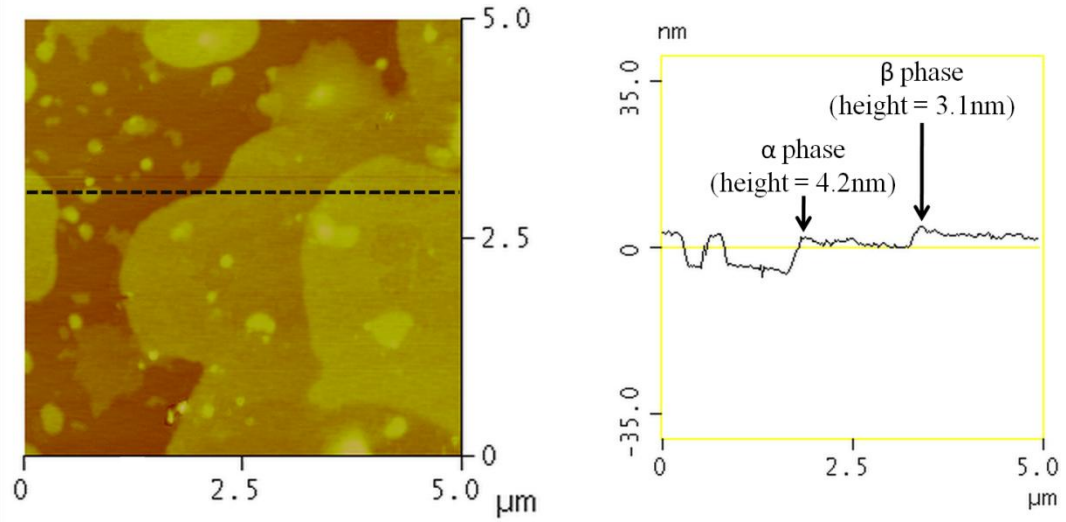

Figure 13. (left) Atomic Force Microscopy (AFM) height image of layered stacking on a film with ts = 16 hours. (right) Height profile of the stacking along the dashed line on left image.

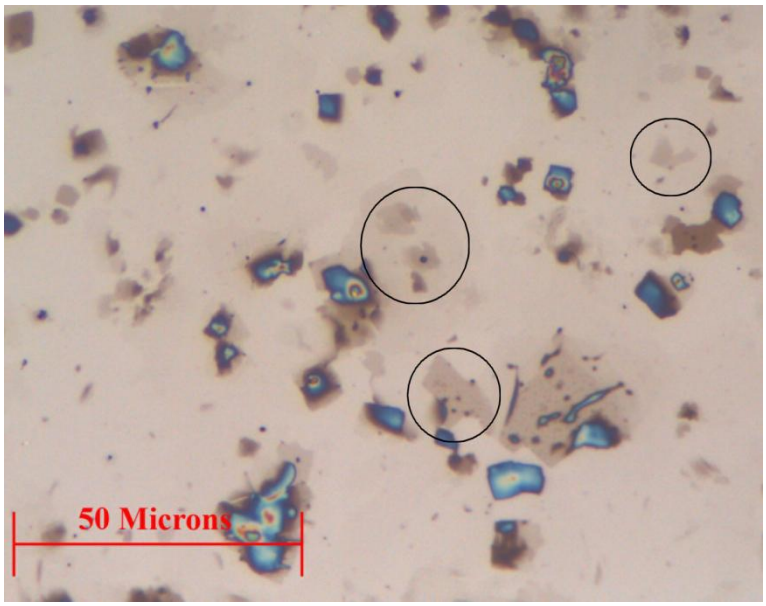

Figure 14. Image of the film surface (tg = 16 hours) captured through optical microscope. Black circles indicate a few locations where layers can be seen.

The layers also can be seen through an optical microscope. In Figure 14 they are illustrated by brown spots, a few of which are circled. The higher is the contrast of those spots, the greater is the number of layers stacked one above the others.

3.4 Fourier Transform Infrared – Attenuated Total Reflectance (FTIR-ATR)

FTIR-ATR is a useful technique to determine the nature of bonds involved in a system. The peaks at 2914 cm^{-1}, 2848 cm^{-1} and 1466 cm^{-1} on Figure 15 were respectively assigned to the asymmetric, symmetric CH_2 stretching modes and CH_2 scissors bending mode (22). The peaks corresponding to the bonds involved in inorganic moieties, Si-O-Si and Si-C are at 1064 cm^{-1} and 794 cm^{-1} respectively. The relative high intensity of the Si-OH peak on Figure 15 (a) and (a') indicates an

incomplete condensation of molecules. This lack of condensation being greater for t_g = 30 minutes than for t_g = 16 hours confirms that short gelation times prevent the molecules from condensing and that the structure is held principally by hydrogen bonds.

After heating up to 300°C, the Si-OH peak totally disappears and the peak corresponding to Si-O-Si bonds has become broader for both gelation times. Therefore, one can guess that the energy brought by the increase in temperature has enhanced the condensation of molecules. All the peaks indicating the presence of alkyl chains (at 2914 cm^{-1}, 2848 cm^{-1} and 1466 cm^{-1}) appear to have a lower intensity on (b') than on (b); this may be explained by the presence of TMOS in the layers which has fewer alkyl groups. Consequently the number of Si-O-Si bonds increases after condensation and the peaks of alkyl chains appear smaller.

After heating up to 800°C, all the C-H peaks involved in alkyl chains disappear which means those chains have cleaved and released between 300°C and 800°C. Since the peaks indicating the presence of Si-O-Si and Si-C remain, one strongly can assume that the energy brought by the higher temperature is strong enough to cause the cleavage of C-C bonds involved in alkyl chains but too low to break the Si-C and Si-O-Si bonds.

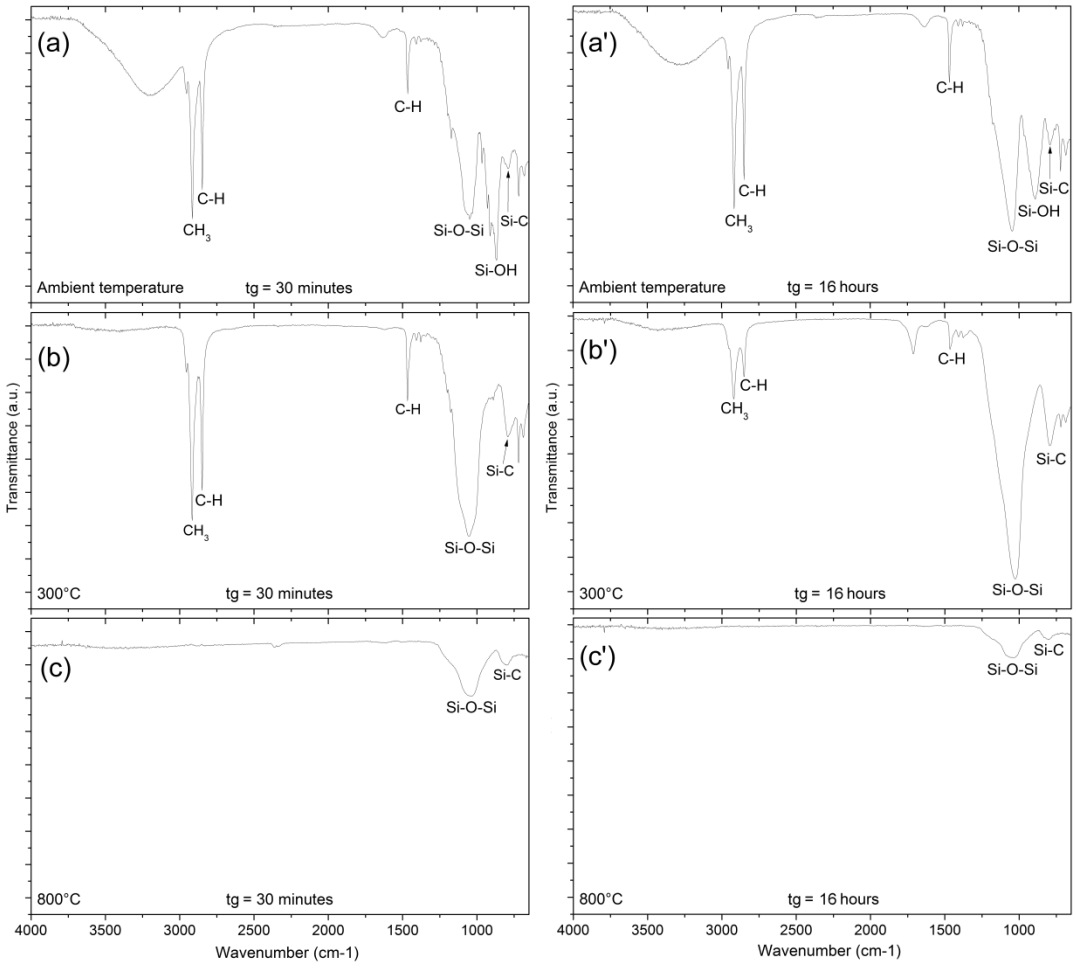

Figure 15. Fourier Transform Infrared – Attenuated Total Reflectance (FTIR-ATR) spectra of HDTMS + TMOS films. (left) tg = 30 minutes, (right) tg = 16 hours. (a) and (a') unmodified films, (b) and (b') after heating up to 300°C and cooling to room temperature, (c) and (c') after heating up to 800°C and cooling to room temperature. Heating and cooling were performed under nitrogen atmosphere.

Indeed, the bond dissociation energy (BDE), which can be defined as a measure of the bond strength in a chemical bond is equal to D° ~ 70 kcal/mol for C-C bonds at 298K (24). This value is lower than the dissociation energies of Si-C and

Si-O-Si bonds which are equal to D° = 94.2 kcal/mol and D° = 136 kcal/mol, respectively, at 298K (25) (26).

3.5 Thermogravimetric analysis (TGA)

TGA curves (Figure 16) have revealed the presence of two main degradations for t_g = 30 minutes at 235°C and 475°C while there is only one main degradation at 475°C for t_g = 16 hours. FTIR-ATR and XRD results have proved that for short gelation times most of the molecules are linked by hydrogen bonds; therefore one can ascribe the degradation at 235°C to the release of molecules which are only weakly bonded (22). This degradation happens at relatively low temperature due to the limited strength of hydrogen bonds which are consequently easier to break.

The second main degradation (at 475°C) often has been cited in literature as being the consequence of the degradation of alkyl chains (27) (28). This feature was confirmed by the FTIR-ATR spectra obtained after heating up to 800°C where only peaks corresponding to the bonds involved into the inorganic network (Si-C and Si-O-Si) appear.

The principal reason why some of the lowest temperature degradations (before 180°C) cannot be seen on the TGA curves obtained on films with t_g = 30 minutes is the peak of the degradation at 235°C which hides some of them. Another reason is the high dependence of films on the conditions in which they have been prepared and analyzed. Therefore this may reveal few insignificant differences in the results.

Moreover, the residual fraction of initial weight is greater for a gelation time of 16 hours than for a gelation time of 30 minutes (~34% for t_g = 16 hours compared to ~9% for t_g = 30 minutes at 700°C). Since at this temperature only the inorganic network of the layers remain, those residual fractions of initial weight indicate that there is more Si-O-Si and Si-C groups for long gelation time. Thus, this partially proved that TMOS molecules have been integrated into the layers and may also confirmed our assumption about the formation of interdigitated layers by the intercalation of TMOS between HDTMS molecules.

Since the boiling point of the solvent (THF) is equal to 66°C, the degradation appearing at 62°C was assigned to the release of this solvent Although the degradation at 112°C was ascribed to the release of water molecules entrapped into the inorganic network, the degradation at 174°C corresponds to the release of water molecules formed during the condensation of some unreacted Si-OH groups (27). Due to DSC and FTIR-ATR analysis made at 90°C (curve and spectrum available in Appendix A), the degradation happening at 90°C could be attributed to an enhancement of the condensation process which creates and releases CH_3OH groups (methanol) (cf. condensation reactions in section 3.1) whose boiling point is equal to ~ 64°C.

Indeed, although FTIR-ATR spectrum indicates a better condensation of molecules at 90°C (lower Si-OH peak and greater Si-C peak), the DSC curve exhibits an exothermic peak at 89°C which designates a structural reorganization in the films at that temperature (condensation).

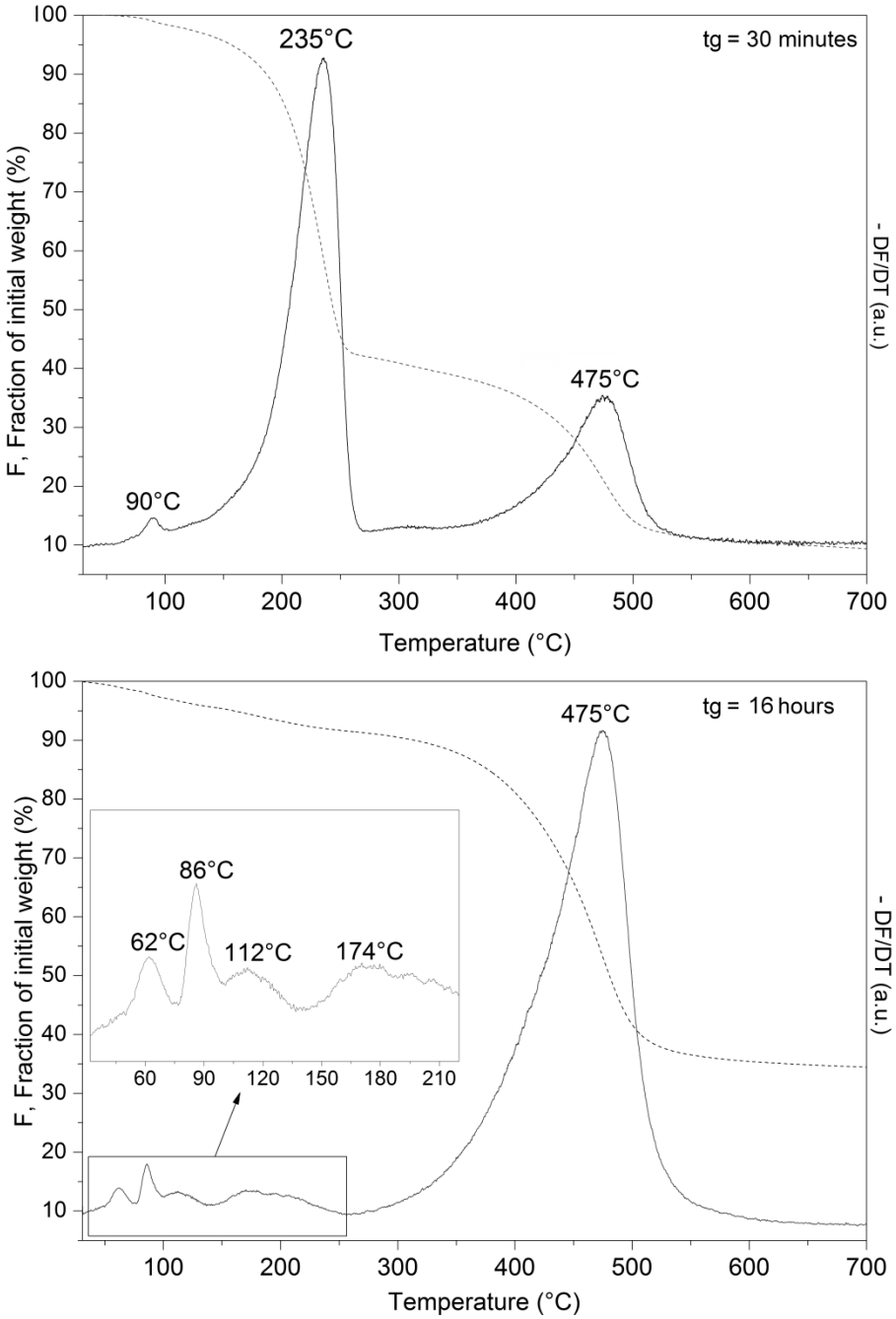

Figure 16. TGA curves recorded on HDTMS + TMOS films, (top) t_g = 30 minutes, (bottom) t_g = 16 hours. The dashed lines correspond to the weight loss trace and the solid lines correspond to the derivative of the fraction of initial weight with respect to time.

3.6 Wettability Tests

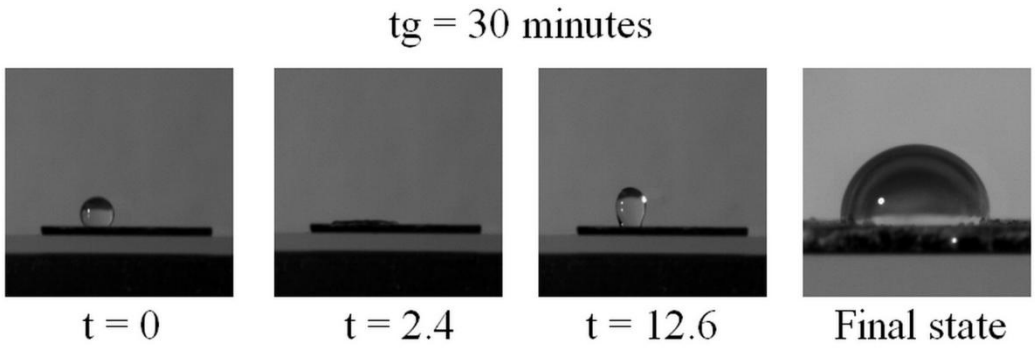

Figure 17. Bouncing of water droplet (diameter = 2 mm) on silicon wafer coated by HDTMS + TMOS film. tg = 30 minutes. The left picture corresponds to the moment when the droplet touches the film. The middle picture corresponds to the moment when the droplet is spread over the film as much as it could. The right image corresponds to the highest point that the droplet can reach after bouncing. The time (t) is expressed in microseconds and the droplet starts its free falling at 4.5 cm above the surface of the film.

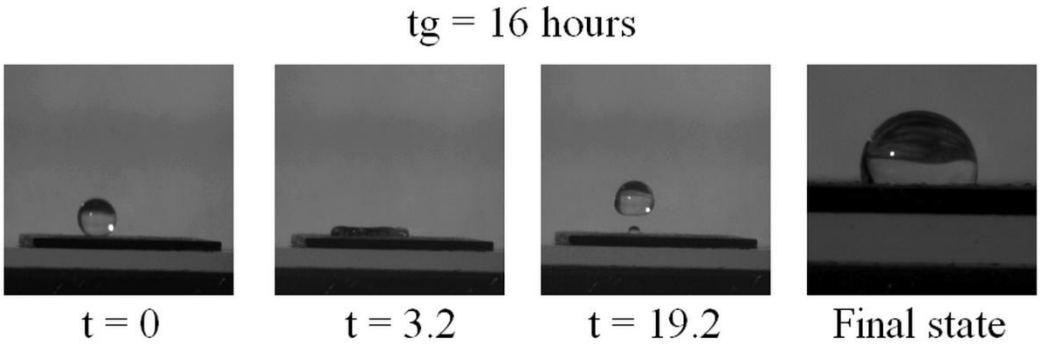

Figure 18. Bouncing of water droplet (diameter = 2 mm) on silicon wafer coated by HDTMS + TMOS film. tg = 16 hours. The left picture corresponds to the moment when the droplet touches the film. The middle picture corresponds to the moment when the droplet is spread over the film as much as it could. The right image corresponds to the highest point that the droplet can reach after bouncing. The time (t) is expressed in microseconds and the droplet starts its free falling at 4.5 cm above the surface of the film.

Figures 17 and 18 show the behaviors of a droplet of water when it bounces on the surface of HDTMS + TMOS films.

When the water droplet reaches its maximum height after bouncing on the surface of film with t_g = 16 hours, it is almost totally disconnected from the film, only a small part remains attached. However, in the case of bouncing on a film with t_g = 30 minutes, a significant part of the droplet remains in contact with the film.

The presence of numerous -OH dipoles due to incomplete condensation in films with a tg = 30 minutes increases the attraction of water to film surface. As we described above, -OH groups are polar, thus in order to minimize the energy, the droplet of water have a tendency to increase its interactions with those groups which is expressed by its spreading over the film. In contrast, less –OH groups in films whose tg = 16 hours reduce the interactions between water and surface, therefore the surface keep only a little part of the droplet during bouncing. In other words, the surface of films whose gelation time is short appears stickier for water.

Nevertheless, since the droplet does not totally spread over the surface, one can assume that the surface of film is either mainly composed of alkyl chains coming from the layers or the proportion of Si-OH groups is too low to get good hydrophilic properties.

It was not possible to determine accurately the final contact angle of the droplets on films; however, one can guess with the naked eye that films with long

gelation time have better hydrophobic properties. Nevertheless the use of silicon wafer as a substrate limits those hydrophobic properties due to its planar surface. Indeed, the roughness of the surface is an important criterion for getting superhydrophobic coatings. A rough surface increases the interfacial area between the film and the droplet which also amplifies the interactions between films and water. Thus, a rough surface may have better hydrophobic properties than flat surface. That is why some papers report remarkable hydrophobic properties of HDTMS coatings on cotton substrates (9). With this type of substrate a contact angle higher than 151° can be achieved.

Obviously, this ability to repel water is a remarkable advantage especially for the protection of electronic devices.

3.7 Summary

This study has uncovered the importance of gelation time as a key parameter for the structural control of nanolayered organosilane films. It has also filled a gap in the knowledge concerning the time dependence of hydrolysis and condensation mechanisms responsible for the formation of highly ordered inorganic-organic hybrid systems by self-assembly.

Since the properties (mechanical, thermal, wettability) of a system are mainly dependent on its internal structure, one can expect to cause their improvement by controlling the molecular arrangement as it has been observed on a preliminary study of the hydrophobic properties on the surface of films.

3.8 Future work

This study has revealed the high potential of the gelation time to control the internal structure of HDTMS + TMOS films. One may envisage it as a starting point for other studies which would be focused on the properties of films depending on their gelation time.

Since this type of films is widely studied, especially for their hydrophobic properties, it could be interesting to continue the investigation of those properties by a dynamic and static study. The dynamic study would be focused on the ways to improve the bouncing of the droplet of water on the surface, and also, an examination of the slipping of the droplet on an inclined surface. The static study would be focused only on the determination of the ways able to improve the contact angle of the droplet on the surface.

Another approach could be the determination of the mechanical properties. Indeed, since the films made from a solution with a long gelation time may have a denser molecular packing due to the presence of interdigitated layers, one can expect them to exhibit better mechanical properties than films made from a solution with a short gelation time. Nanoindentation experiments seem to be the most appropriate way for this type of study.

One can be also interested by the slipping of the layers (turbostratic stacking) when they are still mobile (short gelation time). This behavior could be an interesting way to absorb the energy during a blast shockwave for example. The energy brought

by this blast would lead the mobile layers to slip one relative to the others. After this slipping the molecules still would be able to form new hydrogen bonds with other neighboring molecules. Thus, the energy of the wave would be stored and dissipated by the film.

4 Appendix A

SUPPORTING INFORMATION

This appendix is used for the supporting information of the study. Each of its parts corresponds to a unique type of experimental technique.

4.1 X-Ray Diffraction (XRD)

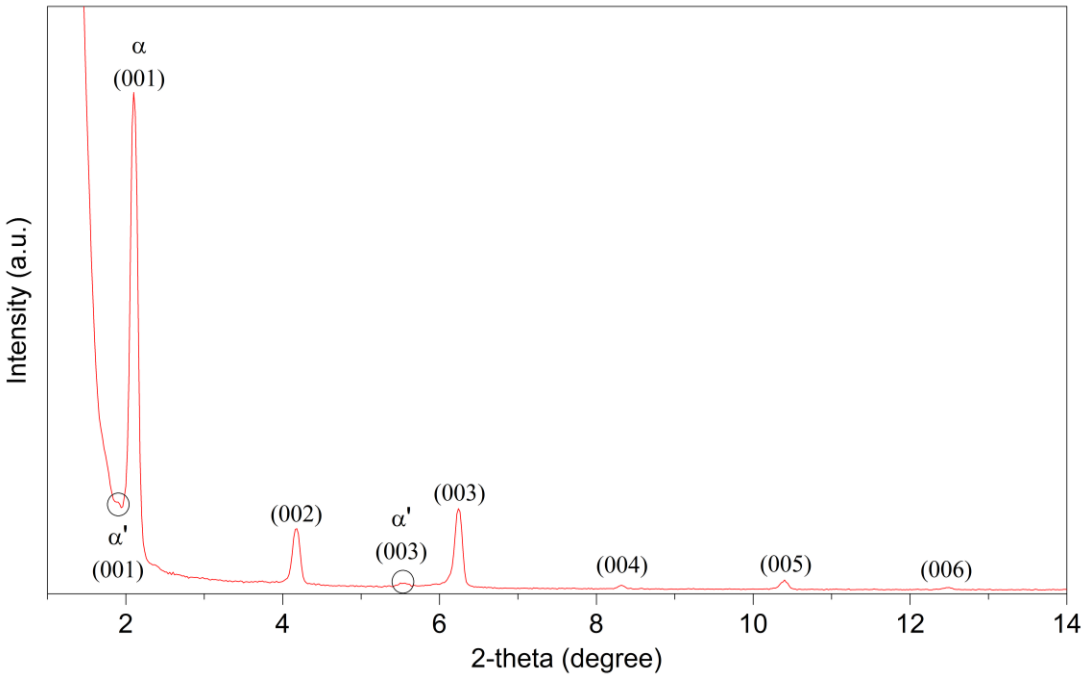

Figure 19. XRD pattern of HDTMS + TMOS thick film for tg = 30 minutes.

The significant thickness of the film used for this experiment causes the presence of two small diffraction peaks corresponding to the α' phase.

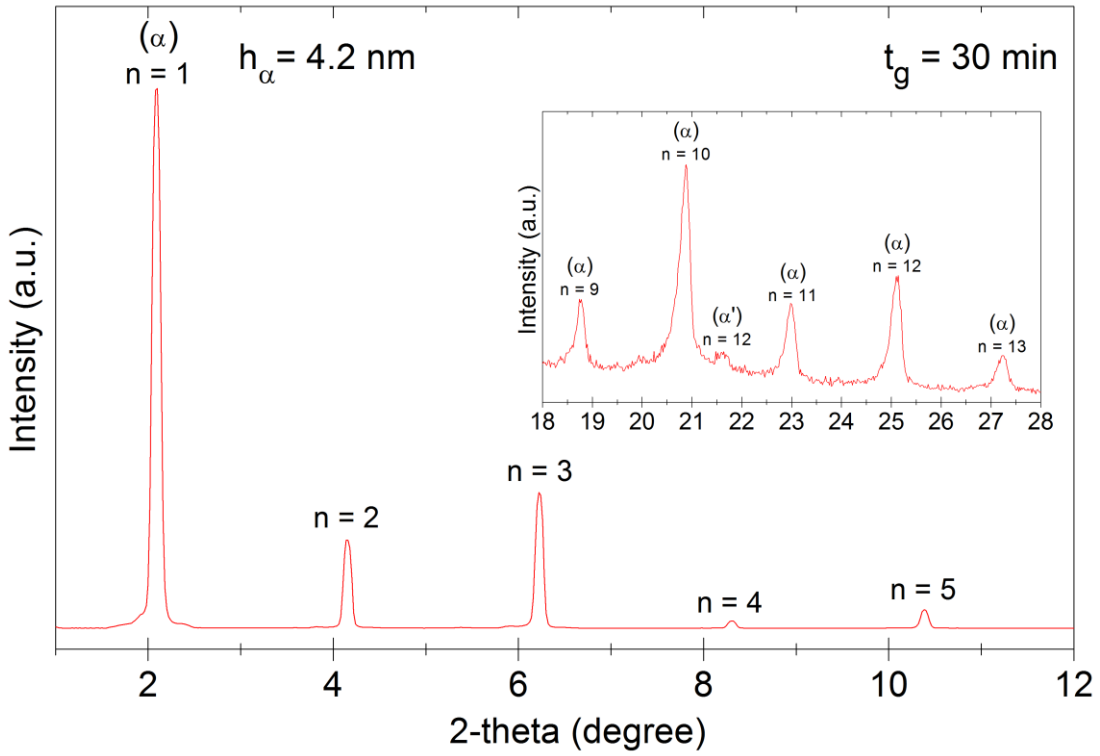

Figure 20. XRD patterns of HDTMS films for tg = 30 minutes. The specimen is composed of a single phase (α) with layer height of hα = 4.2 nm. Inset: wide angle X-ray diffraction peaks.

The XRD pattern in Figure 20 is similar to the one obtained on a film partially composed of TMOS which indicates a comparable nanostructure. The film being too thin one cannot observe the peak corresponding to the spacing between alkyl chains.

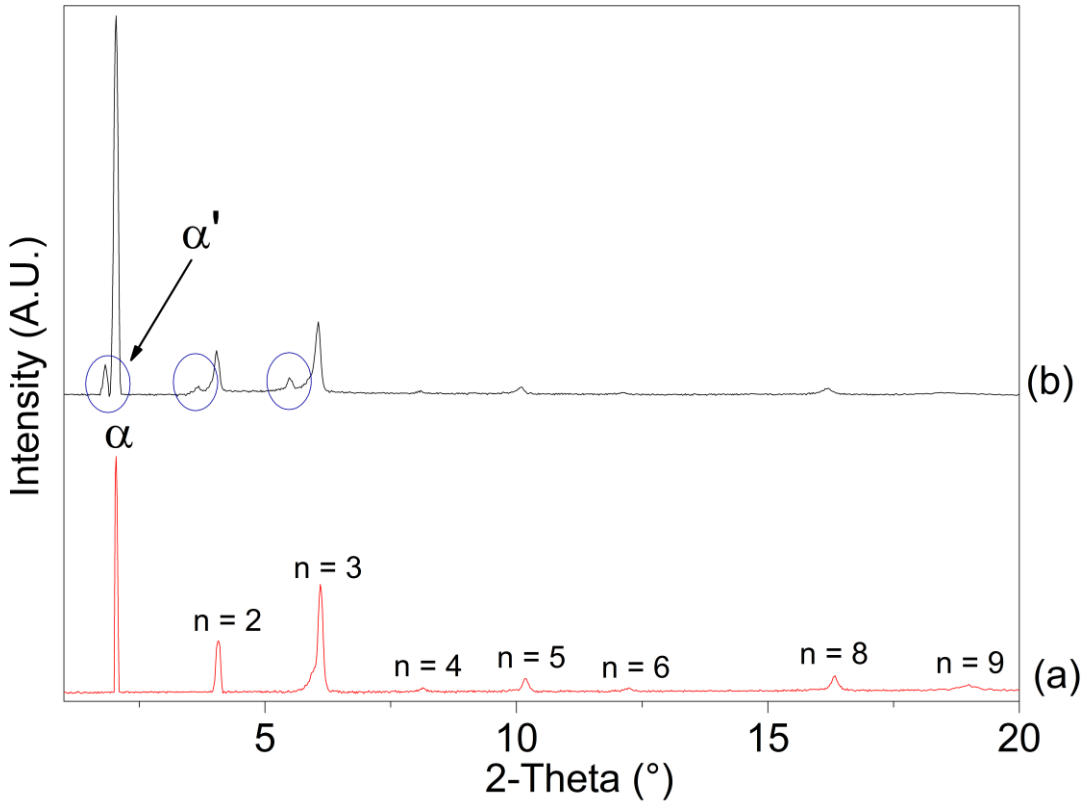

Figure 21. XRD patterns of HDTMS + TMOS film, tg = 30 minutes. (a) Fresh film, (b) Films aged 10 days.

One clearly can see in Figure 21 the appearance of a diffraction peak corresponding to the formation of α' phase in films during the aging.

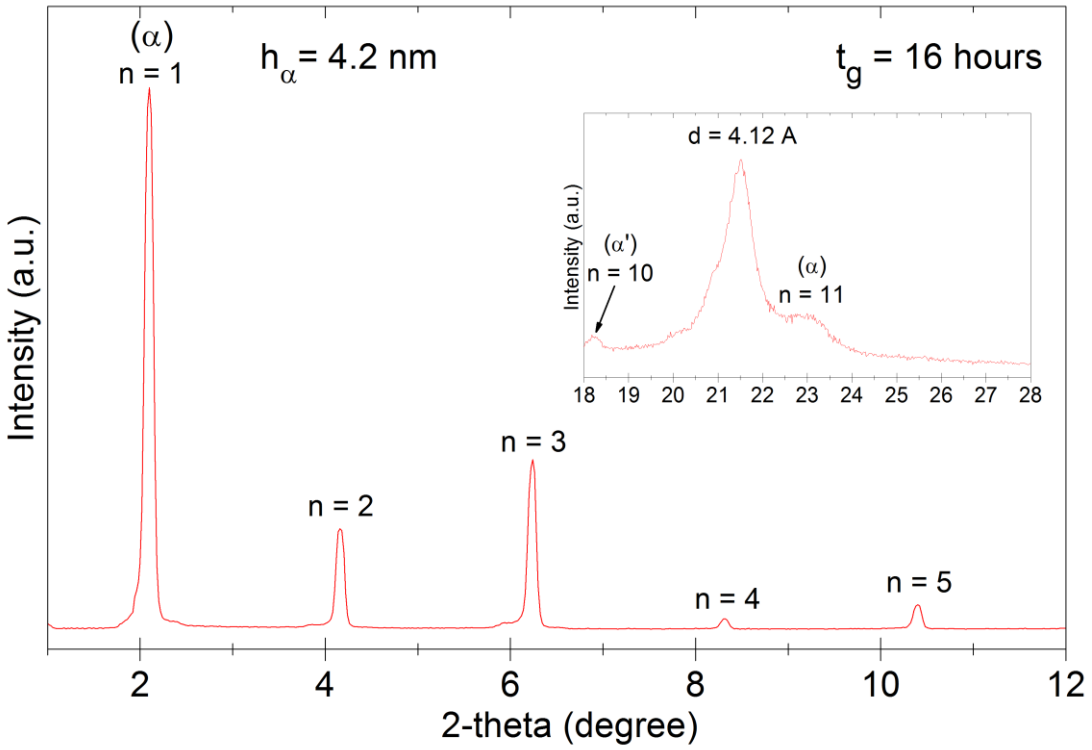

Figure 22. XRD patterns of HDTMS films for tg = 16 hours. The specimen is composed of a single phase (α) with layer height of hα = 4.2 nm. Inset: wide angle X-ray diffraction peaks.

The XRD pattern in Figure 22 is similar to the one obtained on a film made from a solution whose gelation time was equal to 30 minutes. The only difference can be seen on the inset graph which reveals a broad peak at $2\theta \sim 21.2°$ corresponding to the spacing between alkyl chains. The width of this peak indicates that the condensation of molecules has occurred and distorted the inorganic moiety.

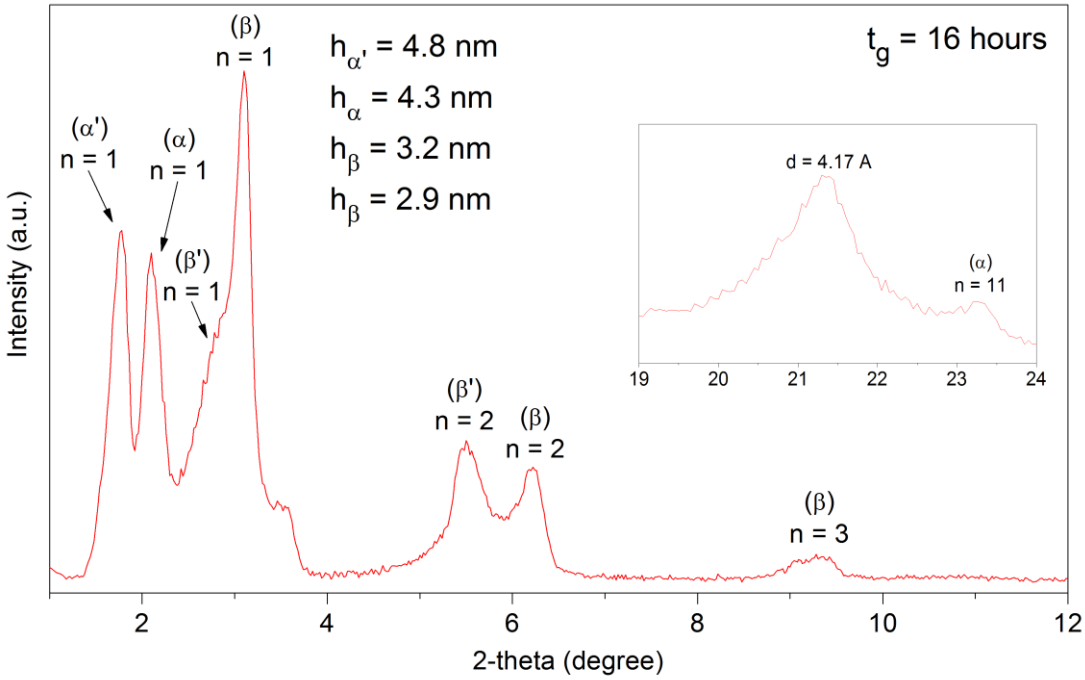

Figure 23. XRD patterns of HDTMS + TMOS films for tg = 16 hours aged 10 days. Multiple phases: α', α, β', β of basal spacing 4.8 nm, 4.3 nm, 3.2 nm and 2.9 nm, respectively. Inset: WAXS shows the presence of two peaks at 2θ ~ 21.2° and 2θ ~ 23°.

Figure 23 shows the result of an XRD experiment performed on a film of HDTMS + TMOS aged 10 days at room temperature and pressure. As one can notice, the internal structure of the film is comparable to the structure of a fresh film.

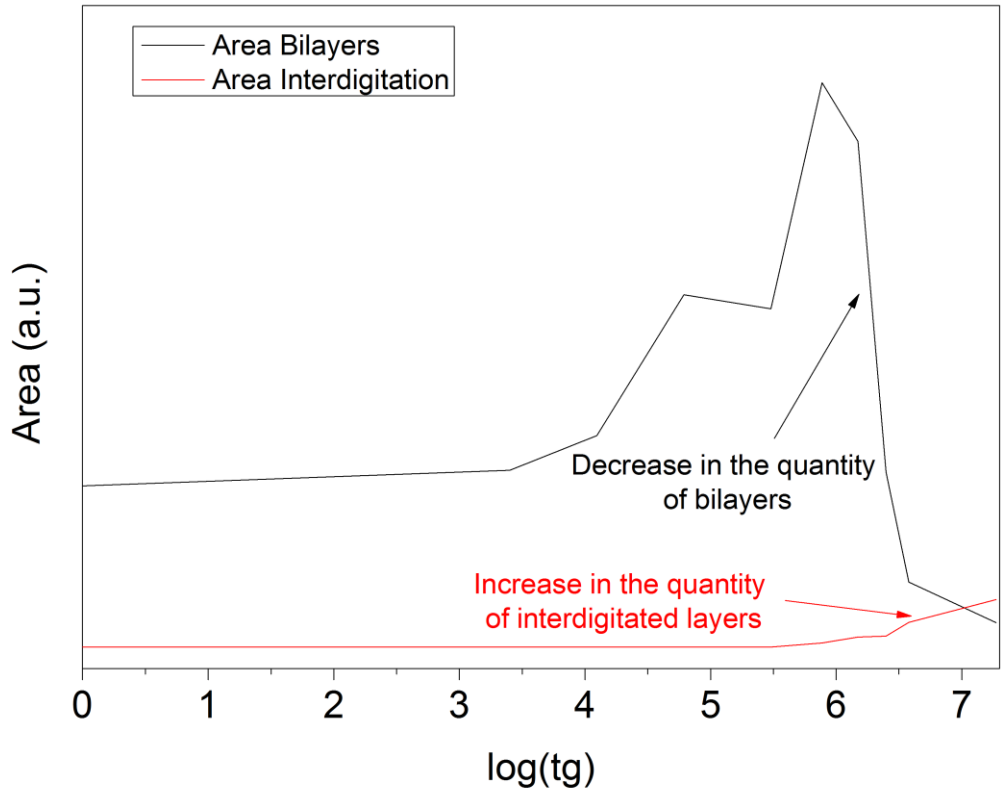

Figure 24. Area under the XRD peaks corresponding to bilayers and interdigitated phases as a function of gelation time (tg).

Even though, the intensity of XRD peaks is dependent on many parameters, such as film thickness and the surface of the specimen covered by the X-Ray beam, which cannot be accurately controlled here. Nevertheless, the graph in Figure 24 may give a rough estimate of the relationship between the enhancement in the formation of interdigitated layers (β and β' phases) and the decrease in the quantity of bilayers (α and α' phases) present in the films.

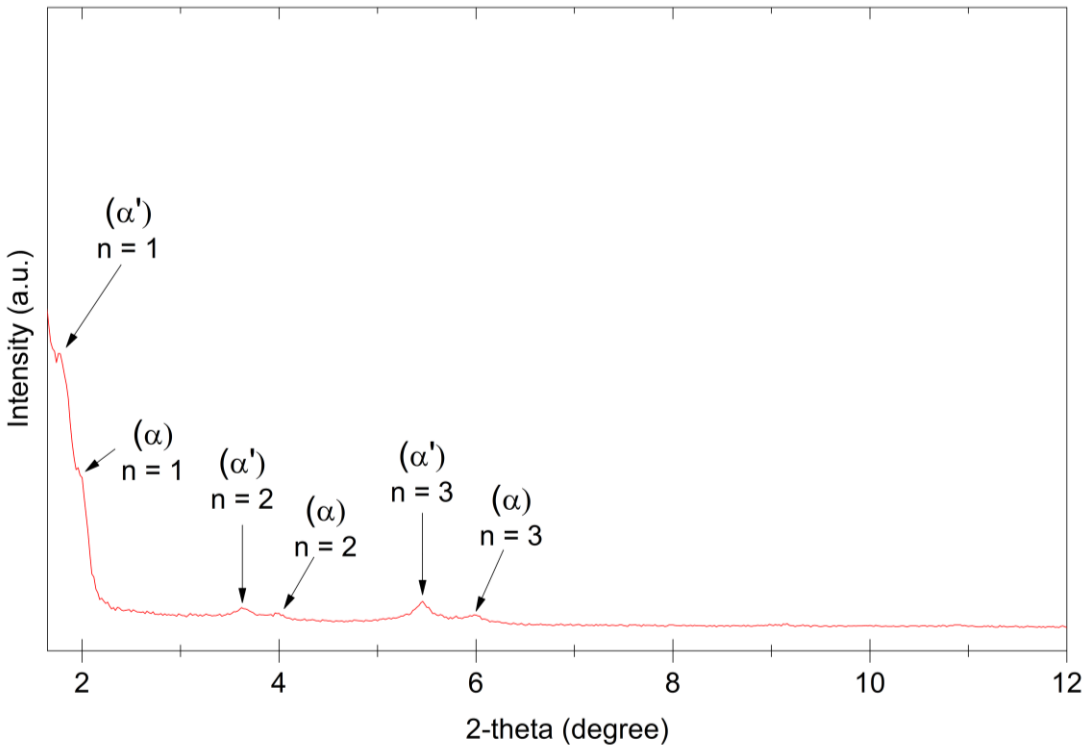

Figure 25. XRD pattern of a film of HDTMS + TMOS. The solution was stored for 48 hours, then TMOS was added followed by a gelation time of 16 hours

The XRD pattern in Figure 25 indicates the presence of bilayers in the film. Since TMOS was inserted in the solution 48 hours after HDTMS, the bilayers had enough time to form and condense. Since the condensation is complete, the structure is locked and TMOS molecules cannot be inserted into the layers.

4.2 Fourier Transform Infrared – Attenuated Total Reflectance (FTIR-ATR)

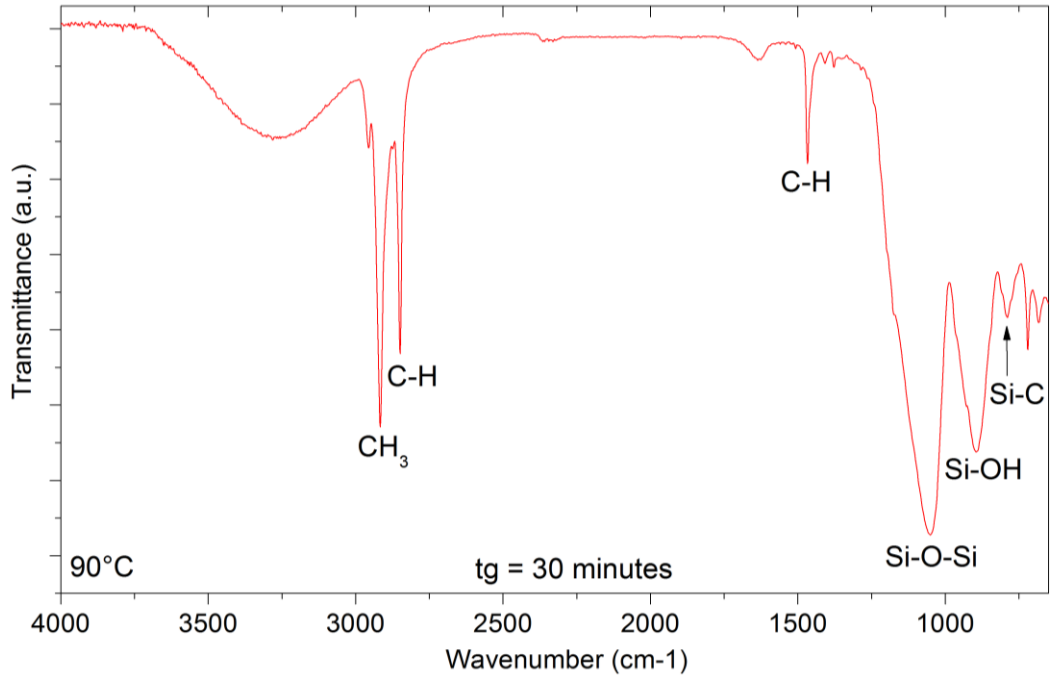

Figure 26. Fourier Transform Infrared – Attenuated Total Reflectance (FTIR-ATR) spectrum of HDTMS + TMOS films after heating up to 90°C and cooling to room temperature. tg = 30 minutes. Heating and cooling were performed under nitrogen atmosphere.

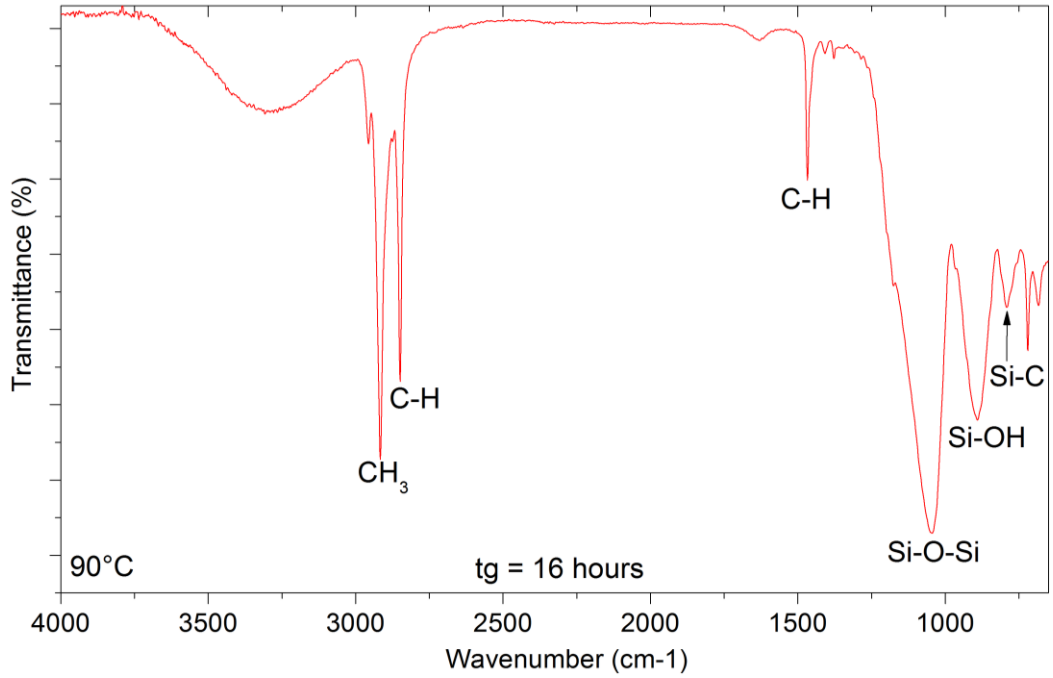

Figure 27. Fourier Transform Infrared – Attenuated Total Reflectance (FTIR-ATR) spectrum of HDTMS + TMOS films after heating up to 90°C and cooling to room temperature. tg = 16 hours. Heating and cooling were performed under nitrogen atmosphere.

On clearly can see on the FTIR-ATR spectra shown in Figures 26 and 27 that the intensity of the Si-OH peak is inferior to the intensity of the Si-O-Si peak. This indicates that the energy brought by higher temperature has enhanced the condensation of molecules which creates CH_3OH groups and therefore may have caused a peak on TGA curves due to the release of methanol.

4.3 Differential Scanning Calorimetry (DSC)

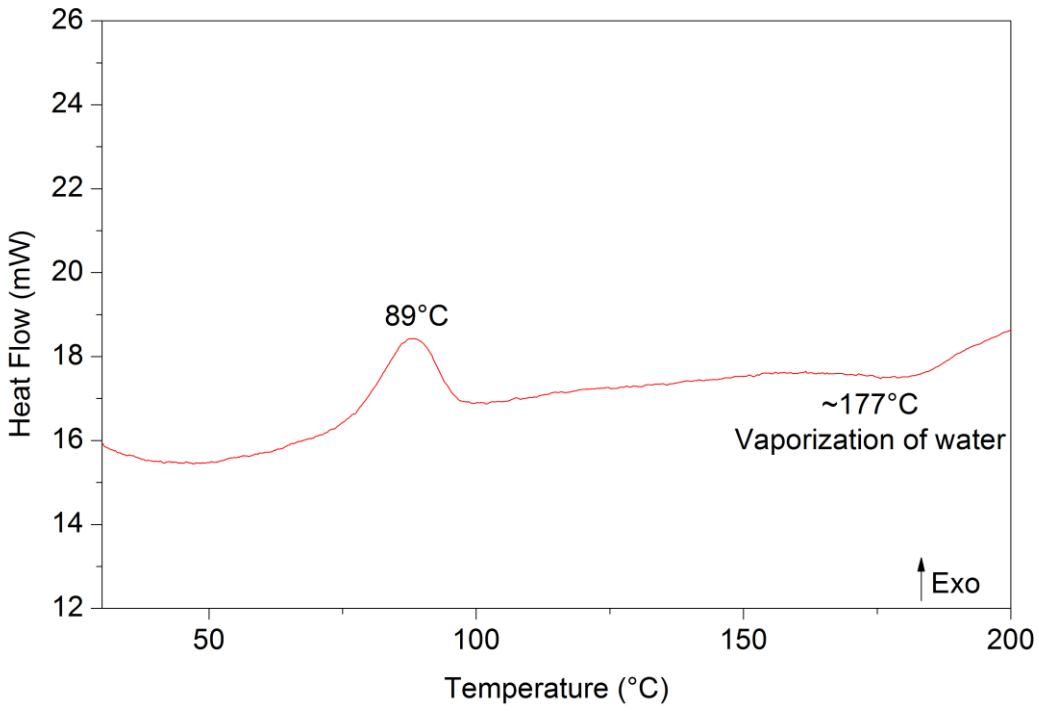

Figure 28. Differential Scanning Calorimetry (DSC) curve of a HDTMS + TMOS film. tg = 30 minutes.

The curve in Figure 28 exhibits two peaks. The endothermic peak at ~177°C was assigned to the release of water molecules entrapped into the inorganic lattice of layers. The exothermic peak at 89°C having no obvious cause, it might be assigned to a sudden condensation of molecules which creates methanol.

5 Appendix B

DETERMINATION OF MECHANISMS RESPONSIBLE FOR THE SELF-ASSEMBLY OF ALKYL-ANTHRACENE MOLECULES

Alkyl-anthracene molecules can be referred to as hydrocarbon compounds. This means they are constituted entirely of hydrogen and carbon atoms. Since this feature does not induce noticeable polarity of molecules, it should prevent the formation of self-assembled thin films. However, we demonstrated the ability of such molecules to build ordered structures without particular preparation or strong modification.

Because this study is still on-going, the results reported in the following parts are preliminary hypotheses only. Therefore it is necessary to state that all of those results are not definite and may be prone to important modifications.

5.1 Introduction

2-Dodecylanthracene (Ant-12) can be classified as an alkyl anthracene molecule because it is constituted of an anthracene group (polycyclic aromatic consisting of three fused benzene rings) to which is added an alkyl chain (sequence of eleven CH_2 groups ended by a CH_3 in the case of Ant-12) (Figure 29).

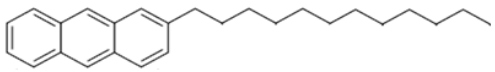

2-Dodecylanthracene (Ant-12)

Figure 29. Molecular structure of 2-Dodecylanthracene (Ant-12).

Contrary to standard molecules used for the formation of self-assembled structures, this molecule does not exhibit a strong polarity. Indeed, the repartition of electron density is roughly uniform throughout the molecule (Figure 30). Therefore, electrostatic interactions should not be considered a feasible method for the formation of ordered films.

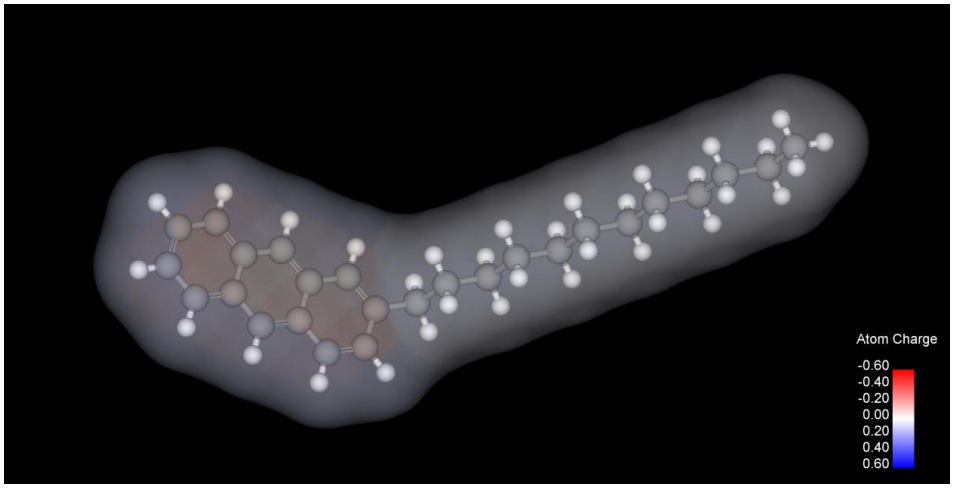

Figure 30. Electrostatic field surrounding an Ant-12 molecule.

The shade surrounding the Ant-12 molecule in Figure 30 indicates a very low intensity electrostatic field localized in the anthacrene group. This can be explained

by a high density of atoms and the presence of double covalent bonds in the anthracene part. One also can notice that the alkyl chain is totally neutral.

If electrostatic interaction is not a sufficient approach for explaining the self-assembly of Ant-12 molecules, then this process must occur by another way. This study focuses on the determination of the mechanisms responsible for the self-assembly of such molecules in order to improve them and establish future applications.

5.2 Experimental section

The linear chemical formula of 2-Dodecylanthracene is $C_{26}H_{34}$ and its molecular weight is equal to 346.5482 $g.mol^{-1}$.

5.2.1 Synthesis

2-Dodecylanthracene was synthesized as a side product during the synthesis of (12-(Anthracen-2-yl)dodecyl)diethoxy(methyl)silane. In a pressure tube, 2-(dodec-11-enyl)anthracene (0.15 g, 0.43 mmole) and diethoxy(methyl)silane 1(0.41 g, 3.1 mmol) were mixed, stirred, and purged with N_2 for 5 minutes. PtO_2 (6 mg, 0.035 mmol) was poured into the tube, and the tube was sealed immediately. The reaction was heated at 80 °C for 18 hours and then cooled down, and the excessive liquids were removed under vacuum. ^{1}H NMR (400 MHz, $CDCl_3$): 8.36 (1H, s), 8.32 (1H, s), 7.96 (2H, m), 7.91 (1H, d, *J* = 8.8 Hz), 7.73 (1H, s), 7.41 (2H, m), 7.31 (1H, dd, *J* = 8.7 and 1.5 Hz), 2.78 (2H, t, *J* = 7.8 Hz), 1.72 (2H, m), 1.44-1.12 (18H, m), 0.85 (3H, t,7.0 Hz). HRFAB: calcd ($C_{26}H_{34}$), 346.2661; found, 346.2662 (29).

5.2.2 Film preparation

Powder of 2-Dodecylanthracene was dissolved into toluene ($C_6H_5CH_3$) maintaining a molar concentration of 3.11 $mmol.L^{-1}$. The solution was sonicated for 1 hour in order to dissolve precipitates and then kept in a refrigerator while not in use. The silicon wafer was sonicated in ethanol for 15 min followed by another 15 minutes in acetone. This wafer was then blown dry with N_2. Thin film was obtained

by spreading and drying a few droplets of the solution onto the silicon substrate for 24 hours in an ambient environment.

5.2.3 Characterization

Wide and small X-Ray diffraction patterns were obtained on a Rigaku D/Max-B Geigerflex diffractometer using a Cu Kα (~1.544 Å) radiation and a graphite monochromator. Digital data were recorded for a 2θ range 1-28° at an angular resolution of 0.02°. The films were analyzed directly on their silicon substrate at an angular velocity of 0.5°/min. Small-angle X-Ray scattering (SAXS) was recorded from 1° to 14° on very thin films. Wide-angle X-Ray scattering (WAXS) was recorded from 18° to 28° on thicker films. The Atomic Force Microscope (AFM) DimensionTM 3100 SPM was used at room temperature to obtain topographic images of the films and highlight the layered structure. Images were recorded at a maximum resolution of 512 samples/line. Differential Scanning Calorimetry analyses (DSC) were performed by a STA 6000 (simultaneous thermal analyzer) from Perkin Elmer through use of an internal reference balance. DSC measurements were made in an appropriate range of temperatures at a heating rate of 5°C/min under air flow. The data were recorded at 0.03°C intervals. Optical and polarized light microscope images were acquired on a Leica DM 2500M. A UV-2401PC UV-VIS made by Shimadzu Instruments was used to record the UV-Vis spectra from 200 to 400 nm at 1.0 nm resolution. The solution was diluted in order to get the best signal.

5.3 Results and discussion

The self-assembly of anthracene-derived molecules is regularly studied especially for their fluorescent (30) (31) and potential electronic properties (29). All those anthracene-derived molecules have at least one functionality, such as a siloxane group (29), which increases the polarity of molecules, and form highly ordered structures due to hydrophobic interactions. However, even though Ant-12 does not have an important polarity, it was noticed that this molecule is able to form ordered structures.

5.3.1 Polarized light microscopy

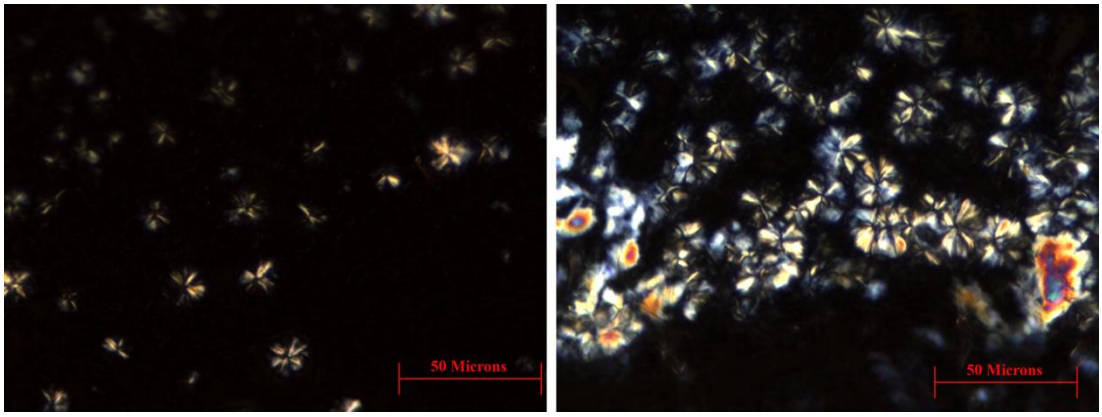

Figure 31. Images of thin film surface observed through polarized light microscope. Pseudo-fan shapes are observable.

As one can see in images in Figure 31, the samples exhibit birefringent properties and a texture very similar to columnar phase (30). The anisotropy of films is expressed under pseudo-fan shapes which indicate where molecules are ordered.

When casted films are thicker, those fan shapes disappear and new dendritic shapes appear (Figure 32).

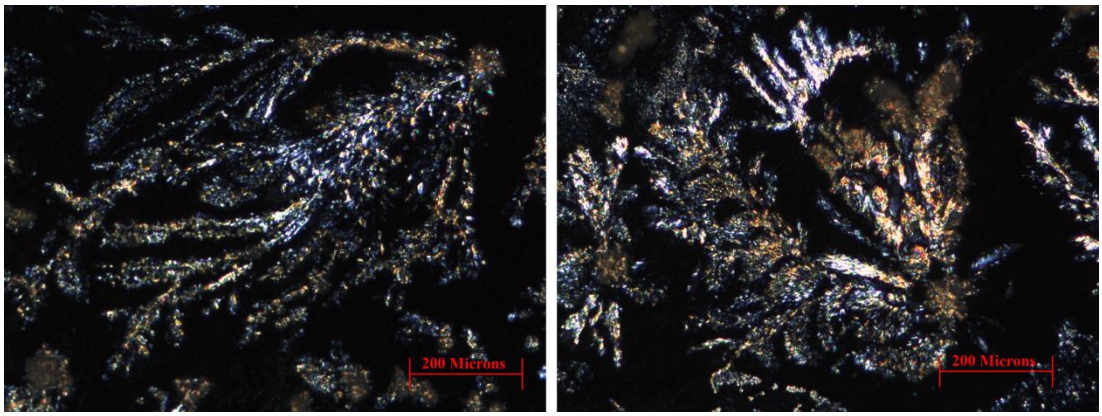

Figure 32. Images of thick film surface observed through polarized light microscope. Dendritic shapes are observable.

Those dendrites seem to grow by following the orientation of the drying (i.e., most of the time from the edge to the center of the substrate). One can clearly see in Figure 32 that all the “arms” of those dendrites come from a unique point. We expect this point to be a defect on the substrate surface where some molecules have accumulated and facilitate other molecules to form ordered structures from this agglomerate.

5.3.2 X-Ray Diffraction (XRD)

Since birefringence properties reveal anisotropy in the materials, an analysis by XRD was completed in order to determine the internal conformation of molecules in the films.

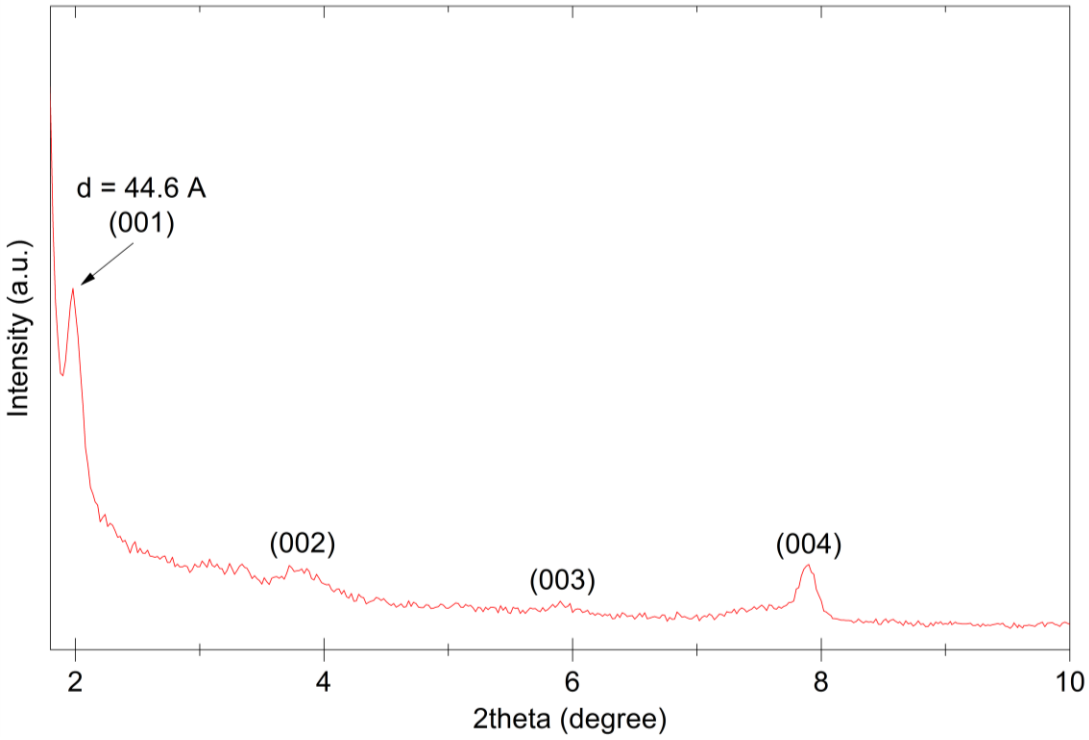

Figure 33. XRD pattern performed on an Ant-12 film. The specimen is composed of a single bilayered phase.

The X-Ray diffraction pattern in Figure 33 exhibits a first diffraction peak which indicates a basal spacing of 44.6 A. Since the length of an Ant-12 molecule is estimated at 21.4 A and can be considered as half of the observed basal spacing, we assigned this basal spacing to the distance created by a stacking of bilayers. The limited number of higher ordered diffraction peaks (up to n = 8) implies that the structure has a limited order. Moreover, WAXS experiments did not reveal any information about the spacing between molecules.

5.3.3 Ultraviolet-Visible Spectroscopy (UV-Vis)

In order to determine the interactions holding the molecular structures, the solution of Ant-12 dissolved in toluene was analyzed by UV-Vis.

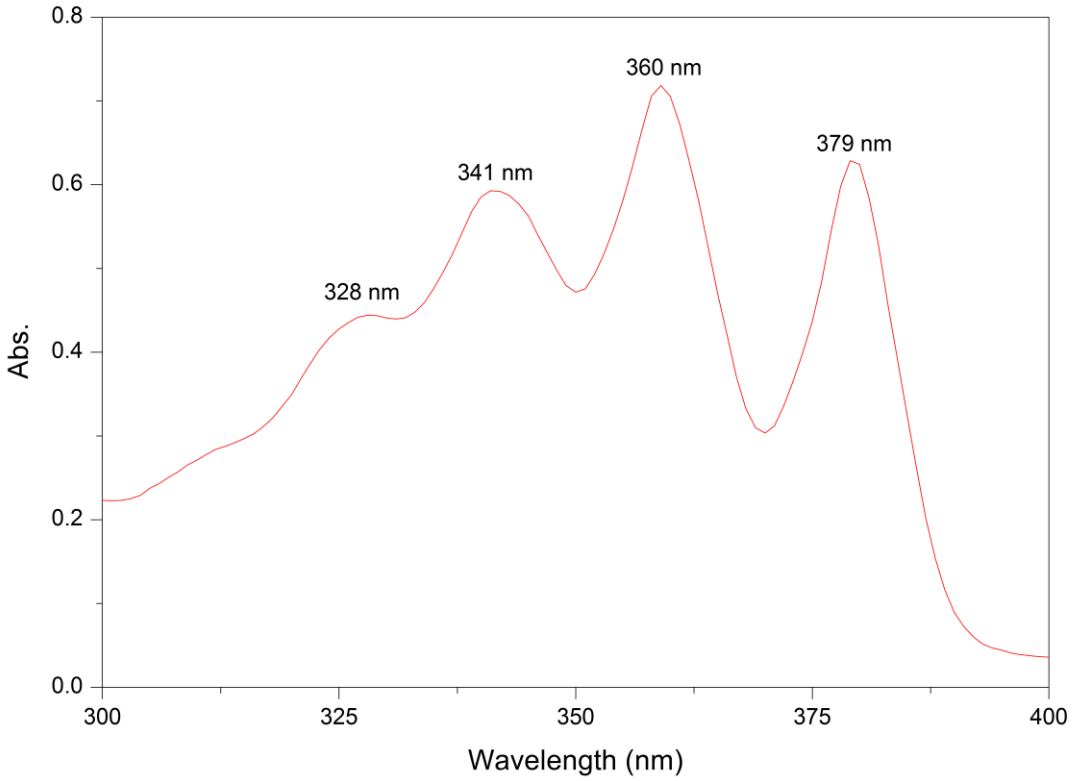

Figure 34. UV-Vis spectrum of Ant-12 dissolved in Toluene. The absorbance peaks are observed at 328, 341, 360, and 379 nm.

UV-Vis spectrum in Figure 34 reveals 4 peaks at 328, 341, 360, and 379 nm. By comparing the values of those peaks with the peaks usually observed on the UV-Vis spectrum of anthracene rings (32) we observed a small shift to a higher

wavelength (~ 4nm) for our peaks at 360 and 379 nm. This shift might be caused by the presence of $\pi - \pi$ interactions (32).

$\pi - \pi$ (or aromatic) interaction is responsible for the stabilization of numerous biological phenomena such as the intercalation of drugs into DNA, but also for the packing of aromatic molecules in crystals (33). Basically this interaction appears between organic compounds containing aromatic moieties and is not so different from other weak bonds such as hydrogen bonds since it is a non-covalent interaction (34).

Even though the exact origins of aromatic interactions are still under investigation and strongly dependent on the geometry of molecules (34) (35), they could be the results of Van der Waals, hydrophobic and electrostatic forces (35).

5.3.4 Differential Scanning Calorimetry (DSC)

DSC analyses were performed in order to determine whether the material undergoes a structural reorganization when temperature is increased. Indeed, the thermal behavior of similar materials already has demonstrated the formation of a better crystalline phase during heating (30).

The presence of exothermic peaks around 90°C may indicate a reorganization of molecules in order to reach a more stable conformation. The fact that this exothermic appears during each heating step signifies that it is inherent to the material and is not coming from a structural relaxation induced by the dropcasting.

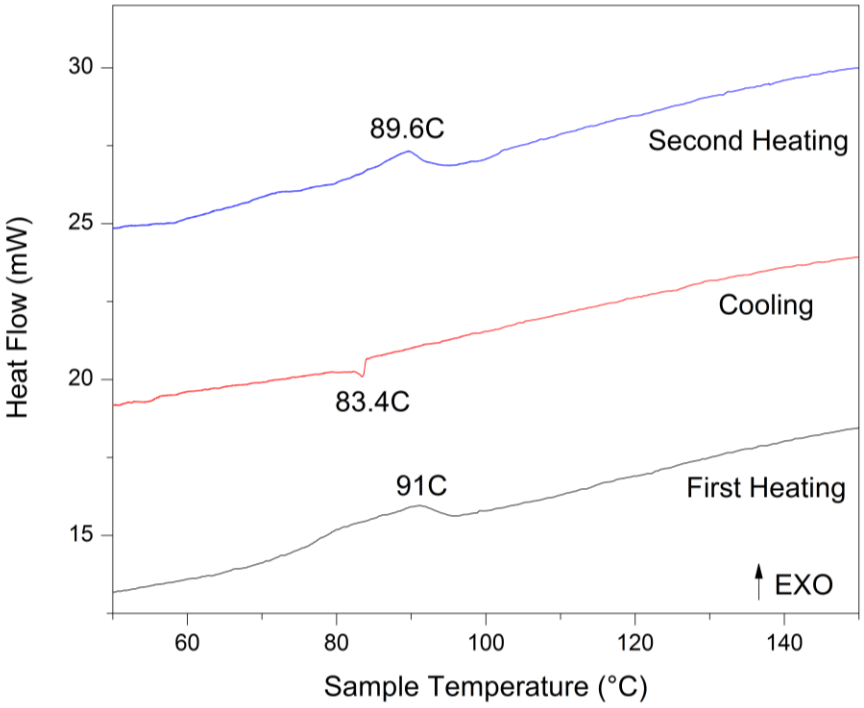

Figure 35. DSC curves obtained on an Ant-12 film. Exothermic phenomena are represented upward. The curves were obtained in 3 steps on the same specimen: first heating up to 200°C (black curve), cooling to 35°C (red curve), then second heating up to 200°C (blue curve).

One can expect this structural reorganization to lead to a stabilization of the structure and better birefringence properties.

The cause of the endothermic peak at 83.4°C is still not well-defined and needs further study.

5.3.5 Atomic Force Microscopy (AFM)

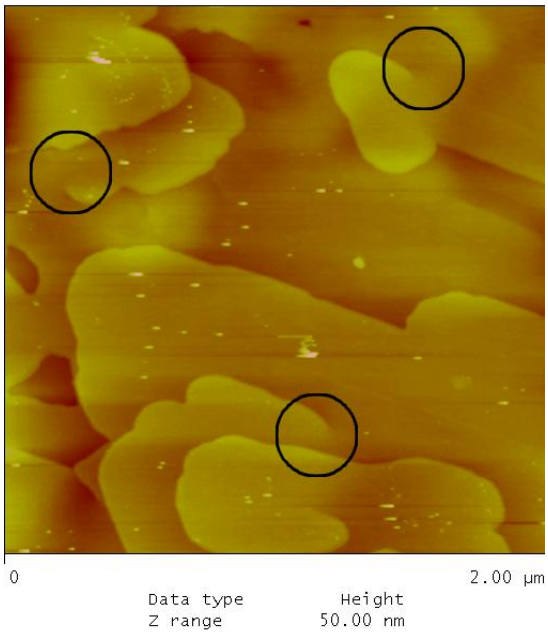

Figure 36. AFM image of the surface of an Ant-12 film.

The AFM image in Figure 36 is of great interest because it depicts an unusual pattern of the layers. Although most of the time layered structures exhibit straight and marked contours, here the layers seem to be formed as a spiral staircase. Thus, the outlines of one layer seem to be merged with the outlines of another, as one can see in the black circles in Figure 36. In some places, the transition between layers is continuous. Further studies are needed here to determine the way of formation of such structures.

5.4 Summary and future work

This preliminary study focuses on the self-assembly of 2-Dodecylanthracene and has demonstrated the ability of this material to form ordered structures and to exhibit unusual structural properties (AFM, DSC). However, according to literature (30), the behavior of Ant-12 films may be compared to liquid crystals.

A modeling of the organization of those molecules should be done in order to clarify the intermolecular interactions leading to the formation of the films.

The temperature dependence of birefringence properties will be investigated by further DSC/TGA studies, and also by real-time observations through a polarized light microscope during the heating of films.

References

[1] Binnig, G.; Rohrer, H.; Gerber, C.; Weibel, E. *Phys. Rev. Lett.* **1982**, *49*, 57.

[2] Liu, S.; Maoz, R.; Sagiv, J. *Nano Letters* **2004**, *4*, 845-851.

[3] Fang, J.; Knobler, C. M. *Langmuir* **1996**, *12*, 1368-1374.

[4] de Boer, B.; Stalmach, U.; van Hutten, P. F.; Melzer, C.; Krasnikov, V. V.; Hadziioannou, G. *Polymer* **2001**, *42*, 9097-9109.

[5] Song, X.; Zhai, J.; Wang, Y.; Jiang, L. *The Journal of Physical Chemistry B* **2005**, *109*, 4048-4052.

[6] Stojanovic, M. N.; de Prada, P.; Landry, D. W. *J. Am. Chem. Soc.* **2000**, *122*, 11547-11548.

[7] Kisiday, J.; Jin, M.; Kurz, B.; Hung, H.; Semino, C.; Zhang, S.; Grodzinsky, A. J. *Proc. Natl. Acad. Sci. U. S. A.* **2002**, *99*, 9996-10001.

[8] Whitesides, G. M.; Mathias, J. P.; Seto, C. T. *Science* **1991**, *254*, 1312-1319.

[9] Li, Z.; Xing, Y.; Dai, J. *Applied Surface Science* **2008**, *254*, 2131-2135.

[10] Hyde, J. F.; DeLong, R. C. *J. Am. Chem. Soc.* **1941**, *63*, 1194-1196.

[11] Kuroda, K.; Shimojima, A. *Mat. Res. Soc. Symp. Proc.* **2002**, *703*, 71-82.

[12] Shimojima, A.; Umeda, N.; Kuroda, K. *Chemistry of Materials* **2001**, *13*, 3610-3616.

[13] Midtiby, H. S. Lipid vesicle. *http://www.texample.net/tikz/examples/lipid-vesicle/* (accessed 06/05, 2010).

[14] Shimojima, A.; Liu, Z.; Ohsuna, T.; Terasaki, O.; Kuroda, K. *J. Am. Chem. Soc.* **2005**, *127*, 14108-14116.

[15] Shimojima, A.; Kuroda, K. *Langmuir* **2002**, *18*, 1144-1149.

[16] Shimojima, A.; Sugahara, Y.; Kuroda, K. *Bull. Chem. Soc. Jpn* **1997**, *70*, 2847-2853.

[17] Bourlinos, A. B.; Ray Chowdhury, S.; Jiang, D. D.; An, Y.; Zhang, Q.; Archer, L. A.; Giannelis, E. P. *Small* **2005**, *1*, 80-82

[18] Hedge, N. D.; Venkateswara Rao, A. *Applied Surface Science* **2006**, *253*, 1566-1572.

[19] Fujimoto, Y.; Shimojima, A.; Kuroda, K. *Chem. Mater.* **2003**, *15*, 4768-4774.

[20] Wolke, R. L. Bond Energy. *http://science.jrank.org/pages/984/Bond-Energy.html*(accessed 06/12, 2010).

[21] Latthe, S. S.; Hirashima, H.; Rao, V. A. *Smart Mater. Struct.* **2009**, *18*, 1-6.

[22] Osman, M. A.; Seyfang, G.; Suter, U. W. *J. Phys. Chem. B* **2000**, *104*, 4433-4439.

[23] Fendler, J. H. *Chem. Mater.* **1996**, *8*, 1616-1624.

[24] Jursic, B. S. *J. Chem. Soc. Perkin Trans. II.* **1999**, 369-372.

[25] Walsh, R. Bond Dissociation Energies in Organosilicon Compounds.*http://www.gelest.com/Library/10BondDiss.pdf* (accessed 06/13, 2

[26] Luo, Y. In *Handbook of Bond Dissociation Energies in Organic Compounds;* Luo, Y., Ed.; Handbook of Bond Dissociation Energies in Organic Compounds; CRC Press LLC: United States, 2003; Vol. 1, pp 362.

[27] Parikh, A. N.; Schivley, M. A.; Koo, E.; Seshadri, K.; Aurentz, D.; Mueller, K.; Allara, D. L. *J. Am. Chem. Soc.* **1997**, *119*, 3135-3143.

[28] De Prado, Luis A. S. A.; Torriani, I. L.; Yoshida, I. V. P. *Journal of Polymer Science: Part A: Polymer Chemistry* **2009**, *48*, 1220-1229.

[29] Jiang, J.; Lima, O. V.; Pei, Y.; Jiang, Z.; Chen, Z.; Yu, C.; Wang, J.; Zeng, X. C.; Forsythe, E.; Tan, L. *ACS Nano* **2010**, null-null.

[30] Olivier, J.; Camerel, F.; Barberá, J.; Retailleau, P.; Ziessel, R. *Chemistry - A European Journal* **2009**, *15*, 8163-8174.

[31] Endo, K.; Ezuhara, T.; Koyanagi, M.; Masuda, H.; Aoyama, Y. *J. Am. Chem. Soc.* **1997**, *119*, 499-505.

[32] Zhang, J.; Lee, J. -.; Wu, Y.; Murray, R. W. *Nano Letters* **2003**, *3*, 403-407.

[33] Hunter, C. A.; Sanders, J. K. M. *J. Am. Chem. Soc.* **1990**, *112*, 5525-5534.

[34] Hunter, C. *Perkin II* **2001**, *2001*, 651

[35] Waters, M. L. *Curr. Opin. Chem. Biol.* **2002**, *6*, 736-741.